A voyage through scales, a missing quadrillion and why the climate is not *what you expect*

S. Lovejoy

Climate Dynamics
Observational, Theoretical and Computational Research on the Climate System

ISSN 0930-7575
Volume 44
Combined 11-12

Clim Dyn (2015) 44:3187-3210
DOI 10.1007/s00382-014-2324-0

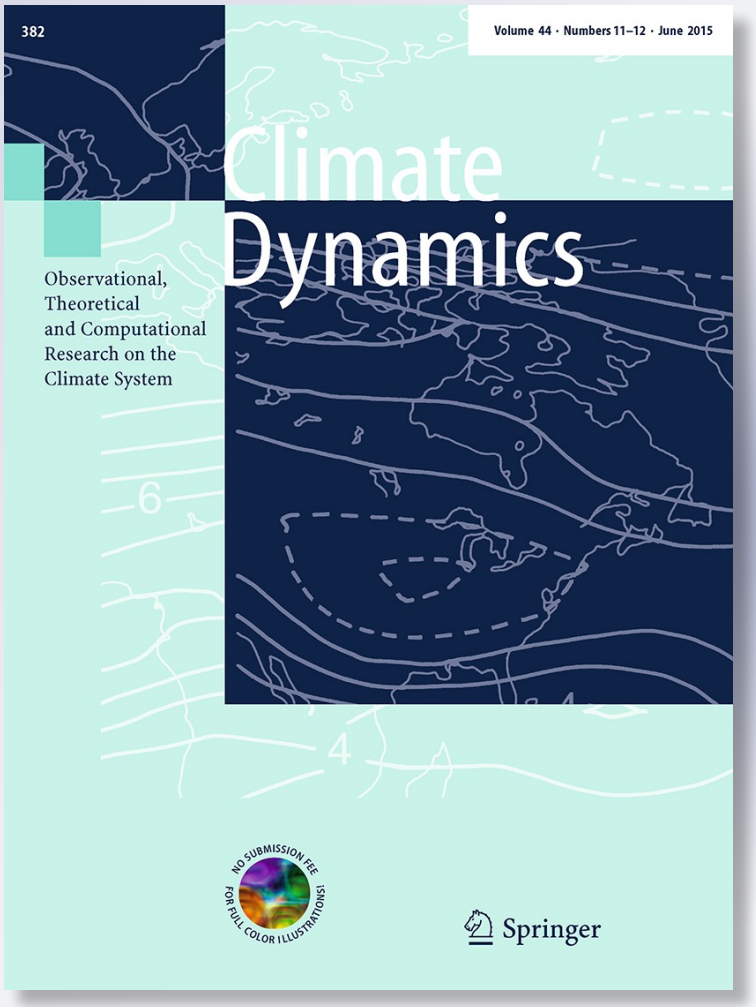

Springer

Clim Dyn (2015) 44:3187–3210
DOI 10.1007/s00382-014-2324-0

A voyage through scales, a missing quadrillion and why the climate is *not* what you expect

S. Lovejoy

Received: 7 February 2014 / Accepted: 3 September 2014 / Published online: 11 October 2014

Abstract Using modern climate data and paleodata, we voyage through 17 orders of magnitude in scale explicitly displaying the astounding temporal variability of the atmosphere from fractions of a second to hundreds of millions of years. By combining real space (Haar fluctuation) and Fourier space analysis, we produce composites quantifying the variability. These show that the classical "mental picture" in which quasi periodic processes are taken as the fundamental signals embedded in a spectral continuum of background "noise" is an iconic relic of a nearly 40 year old "educated guess" in which the flatness of the continuum was exaggerated by a factor of $\approx 10^{15}$. Using modern data we show that a more realistic picture is the exact opposite: the quasiperiodic processes are small background perturbations to spectrally continuous wide range scaling foreground processes. We identify five of these: weather, macroweather, climate, macroclimate and megaclimate, with rough transition scales of 10 days, 50 years, 80 kyrs, 0.5 Myr, and we quantify each with scaling exponents. We show that as we move from one regime to the next, that the fluctuation exponent (H) alternates in sign so that fluctuations change sign between growing ($H > 0$) and diminishing ($H < 0$) with scale. For example, mean temperature fluctuations increase up to about 5 K at 10 days (the lifetime of planetary structures), then decrease to about 0.2 K at 50 years, and then increase again to about 5 K at glacial-interglacial scales. The pattern then repeats with a minimum RMS fluctuation of 1–2 K at ≈0.5 Myr increasing to ≈20 K at 500 Myrs. We show how this can be understood with the help of the new, pedagogical "H model". Both deterministic General Circulation Models (GCM's) with fixed forcings ("control runs") and stochastic turbulence-based models reproduce weather and macroweather, but not the climate; for this we require "climate forcings" and/or new slow climate processes. Averaging macroweather over periods increasing to ≈30–50 yrs yields apparently converging values: macroweather is "what you expect". Macroweather averages over ≈30–50 yrs have the lowest variability, they yield well defined climate states and justify the otherwise ad hoc "climate normal" period. However, moving to longer periods, these states increasingly fluctuate: just as with the weather, the climate changes in an apparently unstable manner; the climate is *not* what you expect. Moving to time scales beyond 100 kyrs, to the macroclimate regime, we find that averaging the varying climate increasingly converges, but ultimately—at scales beyond ≈0.5 Myr in the megaclimate, we discover that the apparent point of convergence itself starts to "wander", presumably representing shifts from one climate to another.

Keywords Climate · Weather · Scaling · Variability · Paleotemperatures

1 Introduction: foreground or background, signal or noise?

One of the most fundamental and striking aspects of the atmosphere is its space–time variability which starts at the size and age of the planet and continues down to millisecond and millimetric dissipation scales. To illustrate this Fig. 1a–e takes a "voyage through scales". Using modern data, it covers over seventeen orders of magnitude from 5.53×10^8 years to 0.07 s (see also R. Rhodes' novel wide

S. Lovejoy (✉)
Department of Physics, McGill University, 3600 University St., Montreal, QC, Canada
e-mail: lovejoy@physics.mcgill.ca

Fig. 1 **a** $\delta^{18}O$ from assemblies of cores from ocean sediments of benthic organisms, Table 1 gives some information on the series. Large values correspond to small temperatures and visa versa. The top series is an update of a global assemblage by Veizer et al. (1999), covering the Phanerozoic; the current geological eon during which abundant animal life has existed and goes back to the time when diverse hard-shelled animals first appeared: this figure goes as far back as this technique will allow. Although 2,980 values were used, but they are far from uniformly distributed; the figure shows a linear interpolation. The corresponding temperature range is indicated based on the "canonical" calibration of -4.5 K/$\delta^{18}O$, and may be as much as a factor 3 too large, see the discussion in Sect. 5.3 (note the negative sign in the calibration: large $\delta^{18}O$ corresponds to small temperatures and visa versa). The middle series is from a northern high latitude assemblage by Zachos et al. (2001) based on global deep-sea isotope records from data compiled from more than 40 Deep Sea Drilling Project and Ocean Drilling Project sites; it has 14,828 values covering the period back 67 million years ago, again non uniformly distributed in time, it is considered to be globally representative. The bottom series is from Huybers (2007), it uses 2,560 data points 12 benthic and 5 planktic $\delta^{18}O$ records over the Quaternary (the recent period during which there were glacials and interglacials; the rough oscillations that are visible, the series is mostly from high northern latitudes). For both of these series a roughly 50 % larger calibration constant −6.5 K/$\delta^{18}O$ was used in order to take into account the larger high latitude variations ("polar amplification" Sect. 5.3). The ellipses, arrows and numbers indicate the parts of the time axis and zoom factor needed to go from one series to the next. This figure is continued in (**b**). **b** The top series is the temperature anomaly from the Epica Antarctic core using a Deuterium based paleotemperature (see Table 1 for information on the data, the temperature anomalies are in degrees K). We may note the loss in resolution (the apparent increase in smoothness) of the curve as we move into the past (to the right); it is an artefact of the compression of the ice column. Clearly, the neat classification of the series into 8 glacial and interglacial (parentheses) epochs is a somewhat subjective simplification of the true variability. Up to at least periods $\approx 10^5$ years, we see that the temperature seems to "wander" i.e. as we consider the change in temperature for increasingly long time periods, the temperature changes more and more. The series in the second row is over the time period indicated by the circle in the top row, it is from a high resolution GRIP core (Summit Greenland). The current interglacial—the Holocene—is at the far left and an ellipse indicates the most recent 1,000 period. This last millennium is indicated in the bottom series which—conversely to the preceding—shows the present on the right, the past on the left. This is a multiproxy temperature estimate from Moberg et al. (2005), the ellipse (*right*) shows the industrial epoch with global warming; not all of this variability is natural in origin. The *ellipses*, *arrows* and *numbers* indicate the parts of the time axis and zoom factor needed to go from one series to the next. This figure is continued in (**c**). **c** The top series the longest available instrumentally based global temperature estimates (monthly, land only, 3,129 values, 1753–2013, Rohde et al. (2013), the red is the annual average (temperatures in °C). The data set goes back to 1753 but due to the very large uncertainties at the early dates (due to limited data), the thickness of the zigzagging at the far left is large. This covers the period since the industrial revolution, which is sometimes known as the anthropocene; the geological period strongly influenced by humans. Starting in 1871, reanalysis data at 2° × 2°, 6 h resolution is available from the 20th C reanalysis (Compo et al. 2011); data at 700 mb are▶ shown. There were over 2×10^5 values so that in order to make the comparisons with the blow-ups in Fig. 1d as fair as possible, we averaged so as to only display 720 points (the resolution of each point displayed here is thus about 3 months). The middle series shows the raw data that includes the dominant annual cycle; the bottom series is the same but with this removed. We also show for reference an estimate the amplitude of the anthropogenic change (from Lovejoy 2014b close to the IPCC AR4 estimate); for the global change since 1880, it is ≈0.85 K. For the land only (top series Rohde et al. 2013), the estimate is 1.5 K. **d** The *upper left* is the same as the lower series in (**c**). We successively take the left half of the series and blow it up by a factor of ≈2, retaining 720 points at each step until we get to the 6 h resolution series (*bottom left*), the total length of each series is *indicated in red*. The *bottom right* series is also from Montreal, but from a millimetre sized thermistor on the roof of the physics building at 0.067 s resolution. The temperature scale is the same for all the series except the lower right. If higher resolution data were available, the variability would continue for at least another 2 orders of magnitude to kHz scales. Starting at the lower left we see that—as for the Epica series (**a**, *top row*)—that the temperature appears to wander like a drunkard's walk with temperature differences $\Delta T = T(t + \Delta t) - T(t)$ tending to grow with time intervals Δt. This character is still apparent at the next (6 h resolution, *lower left*)—at least for intervals as long as 10–20 % of the series length (i.e. up to 10–20 days long). As we move upwards to longer and longer resolutions to the series indicated 34.5 years (which is at 16 day resolution), notice that the overall variation of the series doesn't change much (i.e. the rough range between the maximum and minimum is nearly independent of the resolution). Also notice that the "wandering" character is gradually lost and that by the time we reach a 16 day resolution, fluctuations are tending to cancel in a fairly systematically manner. A consequence is that as move to even lower resolutions (the upper two series), that the amplitude of the fluctuations starts to systematically decrease; we appear to be slowly converging to a well-defined climate state. **e** Representative series from each of the five scaling regimes taken from **a**–**d** with the addition of the hourly surface temperatures from Lander Wyoming, (*bottom*, detrended daily and annually). The Berkeley series (second from the *bottom*) was taken from a fairly well estimated period before significant anthropogenic effects and was annually detrended. The Veizer series (*top*) was taken over a particularly data rich epoch, but there are still traces of the interpolation needed to produce a series at a uniform resolution. In order to fairly contrast their appearances, each series had the same number of points (180) and was normalized by its overall range (the maximum minus the minimum), and each series was offset by 1 K in the vertical for clarity. The resolutions were adjusted so that as much as possible, the smallest scale was at the inner scale of the regime indicated. The series resolutions were 1 h, 1 month, 400 years, 14 kyrs, 370 kyrs and 1.23 Myrs *bottom* to *top* respectively. In the macroclimate regime, the inner scale was a bit too small and the series length a bit too long. The resulting megaclimate regime influence on the low frequencies was therefore removed using a linear trend of 0.25 $\delta^{18}O$/Myr. The resolutions and time periods are indicated next to the *curves*. The *black curves* have $H > 0$, the *red*, $H < 0$, see the parameter estimates in Table 2. From *top to bottom* the ranges used fornormalizing are: 10.1, 4.59, 1.61 (Veizer, Zachos, Huybers respectively, all $\delta^{18}O$), 6.87, 2.50, 25 K (Epica, Berkeley, Lander)

scale range depiction: http://upload.wikimedia.org/wikipedia/commons/f/f5/All_palaeotemps.png). The largest scale is the extreme limit of reliable proxies (but still nearly an order of magnitude less than the earth's lifetime), and the small scale is still more than two orders of magnitude larger than the typical viscous limit.

How can we understand and quantify such huge variability? The first- and until now—the most ambitious

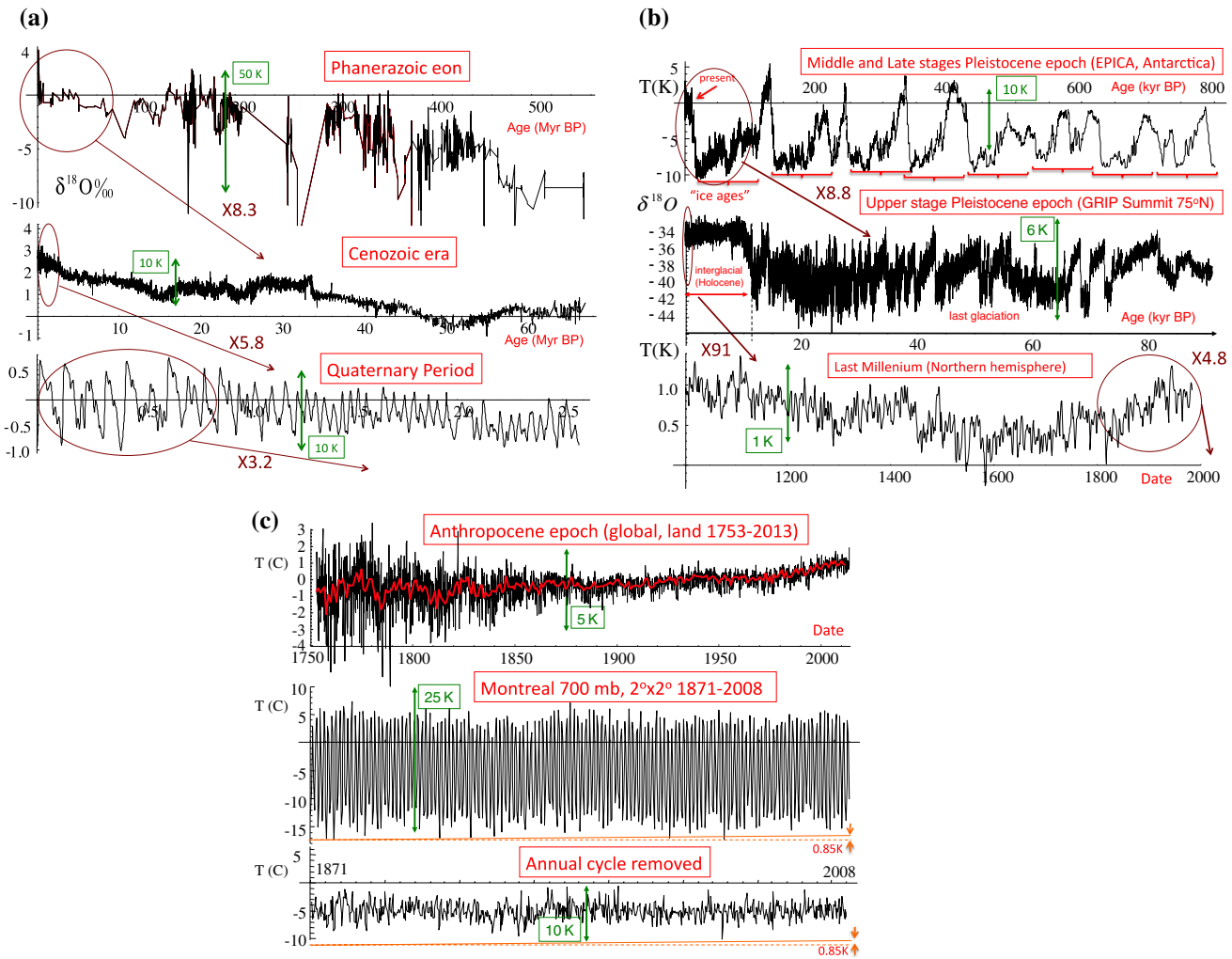

attempt was Mitchell's single composite spectrum ranging from hours to the age of the earth ($\approx 4.5 \times 10^9$ to 10^{-4} years, bottom, Fig. 2a (Mitchell 1976), see also Fig. 2b for a blow-up of the low frequency part). In spite of Mitchell's candid admission that this was mostly an "educated guess", and notwithstanding the subsequent revolution in climate and paleoclimate data, nearly 40 years later it has achieved an iconic status and is still regularly cited and reproduced in climate papers and textbooks (e.g. Dijkstra and Ghil 2005; Fraedrich et al. 2009; Dijkstra 2013). Its continuing influence is demonstrated by the slightly updated version shown in Fig. 2c which currently adorns NOAA's NCDC paleoclimate web site.

Certainly its endurance has nothing to do with its accuracy. Within 15 years, two scaling composites (close to several of those shown in Fig. 2a), over the ranges 1 h to 10^5 yrs, and 10^3 to 10^8 yrs, already showed astronomical discrepancies (Lovejoy and Schertzer 1986; Shackleton and Imbrie 1990 respectively). Whereas over the range 1 h to 10^9 yrs, Mitchell's background varies by a factor ≈ 150, these composites implied that the true range was a factor $\approx 10^{15}$ and Fig. 2a extends this by another order of magnitude. Shackleton and Imbrie (1990) laconically note that their spectral slope was "much steeper than that visualised by Mitchell", a conclusion reinforced by the subsequent scaling composites of Pelletier (1998) and Huybers and Curry (2006). Over at least a significant part of this range, Wunsch (2003) further underlined its misleading nature by demonstrating that the contribution to the variance from specific frequencies associated with specific quasi periodic processes was much smaller than the contribution due to the continuum. NOAA's update (Fig. 2c)—with its totally flat background—compounds Mitchell's error by a further two orders of magnitude bringing it to a total of roughly ten quadrillion. If we attempt to extend Mitchell's picture to the dissipation scales at frequencies 6 or 7 orders of magnitude higher (for millimetric spatial scale variability), the spectral range would increase by an additional ten or so orders of magnitude. Finally, in Fig. 4f, we plot the same information but in real space and find that whereas the

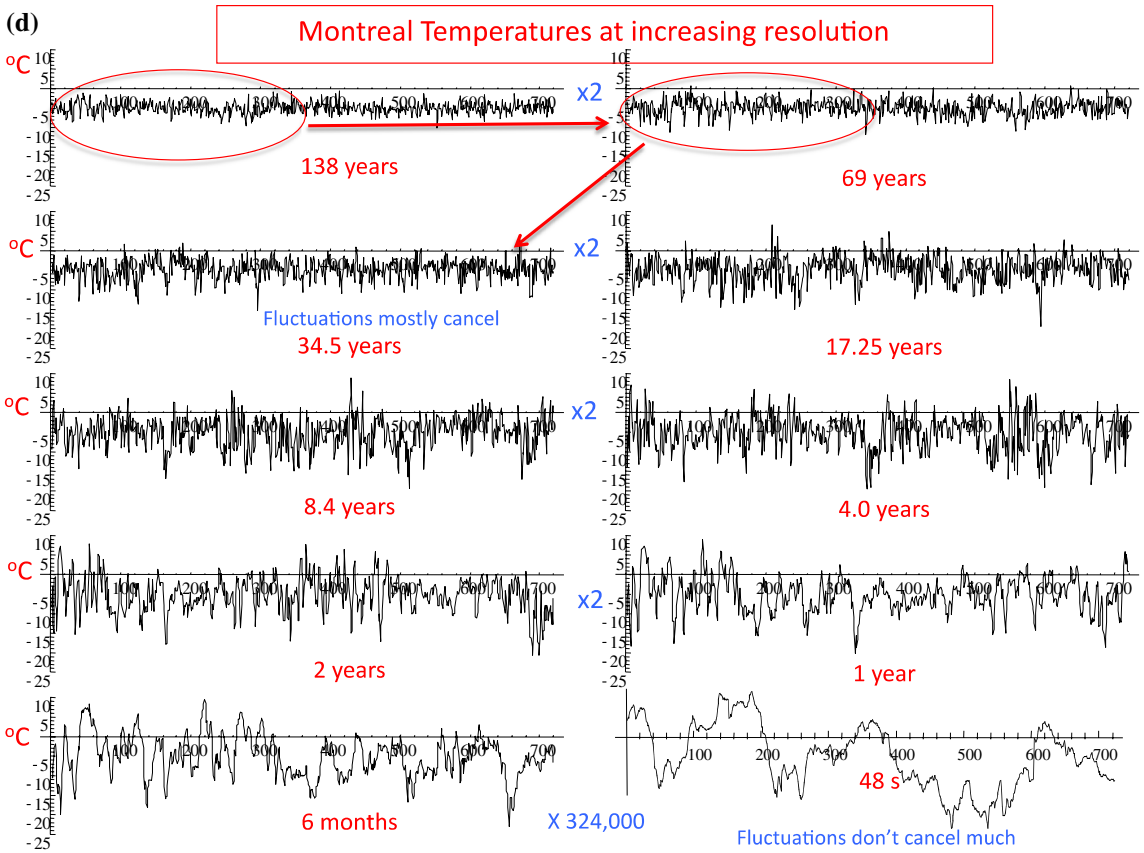

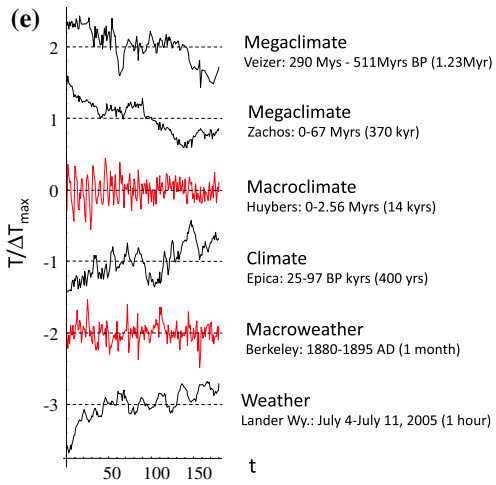

Fig. 1 continued

RMS fluctuations at 5.53×10^8 years are $\approx \pm 10$ K so that extrapolating Gaussian white noise over the range implies a value $\approx 10^{-6}$ K, i.e. it is in error by a factor $\approx 10^7$.

We needn't look far for the reasons for Mitchell's success. In the words of the NOAA site, although "in some respects it over generalizes and over-simplifies climate processes", the "… figure is intended as a mental model to provide a general "powers of ten" overview of climate variability, and to convey the basic complexities of climate dynamics for a general science savvy audience." Just as van Leuwenhook peered through the first microscope and discovered a "new world in a drop of water", NOAA

anticipates finding "new worlds" by zooming in or out of scale. It is an accurate description of what (Mandelbrot 1981) called a "scale bound" scientific ideology: it is so powerful that even quadrillions are insufficient to shake it. And just in case a skeptic fails to see evidence for the purported dominance of oscillations, the site assures us that just "because a particular phenomenon is called an oscillation, it does not necessarily mean there is a particular oscillator causing the pattern. Some prefer to refer to such processes as variability." Variability has thus become synonymous with oscillations, the spectral continuum is beneath consideration.

In Mitchell's time, this scale bound view had already led to an atmospheric dynamics framework that emphasized the importance of numerous processes occurring at well defined time scales, the quasi periodic "foreground" processes illustrated as bumps—the signals—on Mitchell's nearly flat background. Although in Mitchell's original figure, the lettering is difficult to decipher, Fig. 2c spells them out more clearly with numerous conventional examples, and in Sect. 5 we mention a relatively new proposal by Shaviv and Veizer (2003) that the bump at $\approx(135\ \mathrm{Myr})^{-1}$ has a celestial explanation. With the development of low dimensional deterministic chaos, the bumps were increasingly associated with specific chaos models, analysed with the help of the dynamical systems machinery of bifurcations, limit cycles etc., and more recently updated with the help of stochastics: the "random dynamical systems" approach (e.g. Chekroun et al. 2010; Dijkstra 2013). From the spectral point of view, wide range continuum spectra are generic results of systems with large numbers of spatial degrees of freedom ("stochastic chaos", Lovejoy and Schertzer 1998) and hence is incompatible with the usual deterministic chaos. Similarly, the spectra will be scaling—i.e. power laws—if there are no dynamically important characteristic scales or scale breaks. Although in the random dynamical systems approach, the driving noise may be viewed as the expression of a large numbers of degrees of freedom, this interpretation is only justified if there is a significant scale break between the scales of the noise and of the explicitly modelled dynamics, it is not trivially compatible with scaling spectra.

The success of Mitchell's composite climate spectrum parallels that of the earlier meteorological spectral composite in Van der Hoven (1957). The latter figure rapidly became a classic, and for several decades was regularly reproduced (often with embellishments). Notably—in spite of very strong early criticism—it consecrated the scale bound "meso-scale gap" notion that is still used today to justify the (empirically and theoretically untenable) division of atmospheric processes into small scale isotropic 3D and large scale isotropic 2D turbulence (see the discussion in Sect. 3).

The purpose of this paper is therefore to stand Mitchell on his head, to invert the roles of foreground and background—of signal and noise—to treat the spectral continuum with its challenging and nontrivial multifractal scaling, as the fundamental signal and to relegate the residual quasiperiodic processes to the role of background processes where they belong. With the help of scaling exponents, we broadly separate the atmospheric spectrum into five qualitatively different dynamical regimes: weather, macroweather, climate, macroclimate and megaclimate (see Table 2, Figs. 2a, b, 4e). We do not deny the existence of scale bound, quasiperiodic processes, only that they should be properly viewed as perturbations to wide range scaling processes with the latter not the former representing the outcome of the dominant highly nonlinear—but apparently scaling—dynamics. Ironically, the strongest known periodic process—the diurnal cycle—is indeed regularly treated in this way with respect to numerical weather forecasting, all we are suggesting is that the other (much weaker) oscillations be treated similarly.

The time has come to focus our energies on understanding this primary scaling dynamics. By using modern (multiscaling) notions as well as improved (real space) fluctuation analysis techniques (Haar fluctuations), we show that these scaling regimes alternate between those where fluctuations increase with scale (weather, climate, megaclimate) and those where they decrease with scale (macroweather, macroclimate). In particular, we discuss why this distinction is fundamental for understanding—and even objectively defining—the weather and climate. It explains quite simply why—to use the popular phrase—the "weather is what you get" but also why—perhaps surprisingly—the climate is *not* what you expect.

Although evidence for this picture has accumulated for nearly 30 years, the explosion of climate data and paleo data combined with advances in numerical modelling and nonlinear geophysics techniques have lead to rapid progress; we review this literature. This paper amplifies and greatly augments the scope of a recent highly condensed review in the magazine *EOS* (Lovejoy 2013). It benefits from the introduction of improved (interpolation-free) algorithms needed for analysing paleo data ("Appendix"), and applies them to several new data sets; all the figures are original. This includes for the first time its extension to the larger scale macroclimate and megaclimate regimes. It updates earlier reviews (Lovejoy and Schertzer 2012a, 2013) and also contains some new pedagogical material helpful in understanding the fluctuation exponent H (Sect. 2).

In order to lighten the text, some of the technical details and references to the data sets are given in the captions, and the individual series are referred to in a shorthand way, usually by the name of the first author of the relevant source paper, see Table 1.

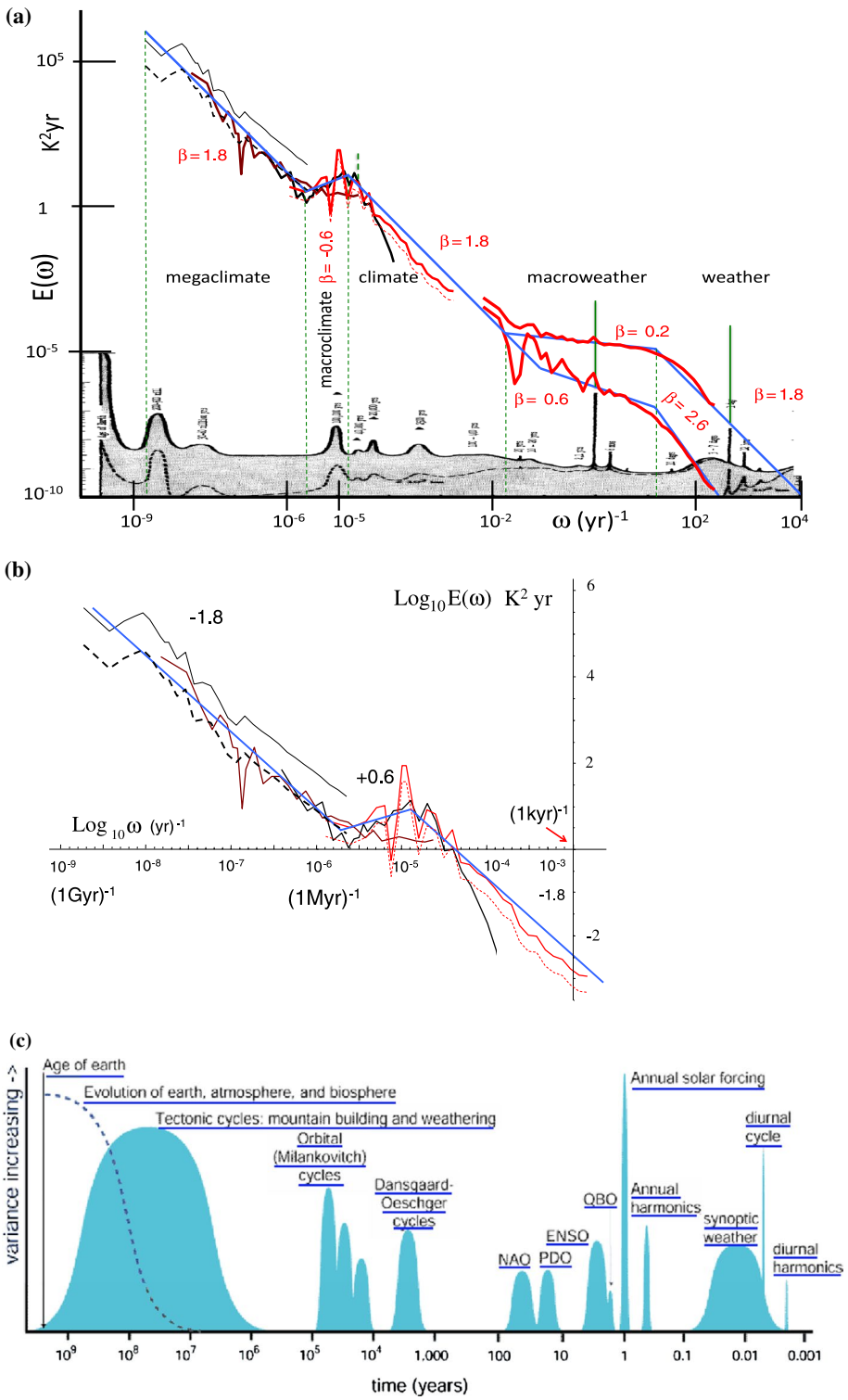

2 Standing Mitchell on his head: the scaling paradigm

Mitchell realized that atmospheric variability existed over a continuum of scales so that the quasiperiodic signals must be superposed onto a continuous "background" spectrum. But he considered the background to be an uninteresting, "noise" which was primarily modelled by the simplest stochastic process—white noise. However, this implies an unrealistically flat spectral background, so that integrals of white noise were also admitted: more precisely Mitchell's model is of a hierarchy of Ornstein–Uhlenbeck processes with spectra $E(\omega) \approx \omega^{-\beta}$ with $\beta = 0, 2$ respectively where

◀**Fig. 2** **a** A comparison of Mitchell's, "educated guess" of the spectrum [*bottom*, Mitchell 1976) with modern evidence from spectra of a selection of the series displayed in Fig. 1 (the plot is log–log). There are three sets of red lines; on the far right, the spectra from the 1871 to 2008 20 CR (at daily resolution) quantifies the difference between the globally averaged temperature (*bottom*) and local averages (2° × 2°, *top*). This figure has been faithfully reproduced many times (with the same admittedly mediocre quality). It is not actually very important to be able to read the lettering near the spikes, if needed they can seen in (**c**) which is inspired by figure **a**. The *upper left red curve* is from the calibrated Epica Antarctic core (interpolated to 276 yrs resolution, see "Appendix"). All the spectra were averaged over logarithmically spaced frequency intervals (10 per order of magnitude), thus "smearing out" the daily and annual spectral "spikes". These spikes have been re-introduced without this averaging, and are indicated by *green* spikes above the *red* daily resolution *curves*. Using the daily resolution data, the annual cycle is a factor ≈1,000 above the continuum, whereas using hourly resolution data (from the Lander series, Fig. 4a), the daily spike is a factor ≈3,000 above the background. Also shown is the other striking narrow spectral spike at $(41\ \text{kyrs})^{-1}$ (obliquity; ≈a factor 10 above the continuum), this is shown in dashed green since it is only apparent in the Huyber series over the period 0.8–2.56 Myr BP. At the *upper left*, the *one brown curve* and *two black curves* are δ^{18}O spectra from the benthic assemblages (Fig. 4c, d), the rightmost *black* is the Huybers series (at 10 kyr resolution), the *middle* (*brown*), is the Zachos series (interpolated to 18 kyrs), the *leftmost* (*black*) is Veizer series (interpolated to 185 kyrs). For the global (not polar) Veizer series, the canonical calibration $-4.5\ \text{K}/\delta^{18}\text{O}$ was used for the *upper solid line*, the (*extreme*) tropical ocean value $-1.5\ \text{K}/\delta^{18}\text{O}$ was used for the *solid line* (the true calibration is presumably between the two; see the discussion in Sect. 5.3), the caption of Fig. 4c, d and see the blow-up in (**b**) for the northern and high latitude Huybers and Zachos series the calibration $-6.5\ K/\delta^{18}\text{O}$ was used, this aligns best with the Epica ice core data (here and Fig. 4c) and is justified by the roughly 50 % higher high latitude variability; this single calibration constant is the only "adjustable" parameter in the figure (the *dashed red line* shows the Epica spectrum with the downward shifted by a factor $(1.5)^2$ to take into account the high latitude amplification). Beyond this direct calibration factor, small additional vertical shifts are required because of intermittency: when comparing the spectra of a process averaged at resolutions differing by a factor λ, the spectral densities will be in ratio $\lambda^{K(2)}$ where $K(2)$ is of the order of 0.1–0.2 in the megaclimate regime (Table 1; see Gagnon et al. 2006) for the theory: the *Zachos curve* was displaced downward by 0.25, and the Veizer curve by 0.45 so as to make their resolutions effectively comparable with the *Huybers curve*). The final adjustment was to give the 20CR spectra a small (0.2) shift downward to account for the fact that for technical reasons it was taken at the slightly more variable vertical level of 700 mb rather than the surface (the shift was estimated from Fig. 4a by comparing it with the RMS surface series fluctuations). To avoid crowding, the spectra of the other series analysed in Fig. 4 were not shown. The *blue lines* have slopes indicating the scaling behaviours ($E(\omega) \approx \omega^{-\beta}$) deduced from the real space Haar analyses (Fig. 4). The scaling exponents β are related to the slopes in Fig. 4 (ξ(2)/2; see Table 2) by $\beta = 1 + \xi(2)$. The *thin dashed green lines* show the transition frequencies deduced from the spectra; these are at $(20\ \text{days})^{-1}$, $(50\ \text{yrs})^{-1}$, $(80\ \text{kyrs})^{-1}$, and $(500\ \text{kyrs})^{-1}$ close to those deduced in real space in Fig. 4. At the far right, the *blue line* is close to the detrended hourly Lander data, the exponent is the turbulent value $\beta = 1.8$ (and hence presumably continues down to much higher frequencies). **b** A blow up of the low frequency spectra in (**a**) *upper left*, *black*, Veizer (*solid* $-4.5\ \text{K}/\delta^{18}\text{O}$, *dashed*, $-1.5\ \text{K}/\delta^{18}\text{O}$), *upper left brown*, Zachos, *intermediate*, *black*, Huybers ($-6.5\ \text{K}/\delta^{18}\text{O}$) and *rightmost, red*, Epica (the *dashed red line* is shifted downward by a factor $(1.5)^2$ to compensate for high latitude amplification). The reference *lines* have the slopes indicated, the transitions are at $(80\ \text{kyrs})^{-1}$, $(500\ \text{kyrs})^{-1}$. Note the bump in the *Veizer curve* at around $(1.35\ \text{Myr})^{-1}$, this has been hypothesized as a consequence of periodic cosmic ray flux forcings (Shaviv and Veizer 2003). **c** The updated version of Mitchell's spectrum reproduced from NOAA's NCDC paleoclimate web site (http://www.ncdc.noaa.gov/paleo/ctl/about1.html). The "background" on this paleo site is perfectly flat; hence in comparison with the empirical spectrum in (**a**), it is in error by an overall factor $\approx 10^{16}$

β is the spectral exponent: the negative slope on the log–log plot in Fig. 2a. The spectral spikes—whose apparent importance is artificially magnified by the grossly depleted "background"—are therefore superposed on a spectrum consisting of a series of "shelves" and represented distinct physical processes. Mitchell explained his idea as follows:

> As we scan the spectrum from the short-wave end toward the longer wave regions, at each point where we pass through a region of the spectrum corresponding to the time constant of a process that adds variance to the climate, the amplitude of the spectrum increases by a constant increment across all substantially longer wavelengths. In other words, each stochastic process adds a shelf to the spectrum at an appropriate wavelength (Mitchell 1976).

Interestingly, Fig. 2a shows that Mitchell did a much better job at estimating the amplitude of the sharp spikes although there were still biases in the "bumps". For example from the red daily resolution curve, the annual cycle is a factor ≈1,000 above the background (the green spike added to the global spectrum on the right of Fig. 2a) compared to Mitchell's estimate of a factor ≈400, and Mitchell's daily spike is about a factor ≈80 above the background whereas the hourly Lander data has a spike nearly a factor ≈3,000 above the background (Lovejoy and Schertzer 2013). As for his "bump" near $(10^5\ \text{years})^{-1}$, it is a factor ≈10 above the background which is about the same as that from the Huybers and Epica spectral estimates. However even here his scale-bound bias is apparent since the width of this "bump" is roughly a factor of two in frequency which is much less than the true width (a factor of ≈10); in Sect. 5.3, we argue that rather than being a quasiperiodic signal, this may simply be a short macroclimate scaling regime with $H < 0$.

By the early 1980s, following the explosion of scaling (fractal) ideas it was realized that scale invariance was a very general symmetry principle often respected by nonlinear dynamics, including many geophysical processes and turbulence. The signature of a scaling process is a power law spectrum, linear on a log–log plot. Although in order to accommodate the wide range of scales, Mitchell had found it "necessary to resort to logarithmic coordinates",

Table 1 Some characteristics of the paleo data series used in this paper

Short hand series name	Data type	Range	Region	No of data point	Comments	Reference
Veizer	Benthic $^{18}\delta O$	553 Myrs	Global excluding Antarctic	2,980	Relation to temperature is under debate	Veizer et al. (1999)
Zachos	Benthic $^{18}\delta O$ 40 DSDP and ODP sites,	67 Myrs	high latitudes	14,825	In last 35 Myr, relation to temperature is indirect through ice sheet formation	Zachos et al. (2001)
Huybers	Benthic $^{18}\delta O$	2.56 Myrs	Mostly northern, not polar	2,560	Partially due to ice sheets, partially temperature	(Huybers 2007)
Epica	Deuterium	800 kyrs	Antarctic	5,788		(Schwander et al. 2001)
GRIP 55 cm	Ice $^{18}\delta O$	248 kyrs	Greenland	5,425	Sampled at 55 cm vertical resolution	NCAR/EOL under sponsorship of the National Science Foundation. http://data.eol.ucar.edu/
GRIP high resolution	Ice $^{18}\delta O$	91 kyrs	Greenland	17,551	Roughly constant sampling at $\approx$5.2 year resolution	Data courtesy of P. Ditlevsen
Vostok	Deuterium	420 kyrs	Antarctic	3,312	Sampled at 1 m vertical reoslution	ftp.ncdc.noaa.gov/pub/data/paleo/icecore/antarctica/vostok/deutnat.txt
Moberg	multiproxy	1000–1979	Northern hemisphere	979	See Fig. 1b, this is one of the three multiproxies analysed in Fig. 4a	Moberg et al. (2005)
Huang	Boreholes and proxies	1500–1979	Northern hemisphere	479	See Fig. 4a	Huang (2004)
Ljundqist	multiproxies	0–2000	Northern hemisphere	200	Only data from 1500 to 1979 were used in Fig. 4a	Ljungqvist (2010)

Table 2 The five atmospheric scaling regimes with their approximate inner scales and their basic temporal scaling exponents H, C_1, α as well as the derived spectral exponent $\beta = 1 + \xi(2)$

	Weather[a] (local)	Weather[a] (global)	Macroweather (local)[b]	Macroweather (global)	Climate[c]	Macroclimate[d]	Megaclimate[e]
Inner scale	≈1 ms	–	≈10 days	10 days	≈40 years	≈80 kyrs	≈0.5 Myr
H	0.4	0.75	−0.4 to −0.2	−0.2	0.4	−0.8	0.4
C_1	0.08	0.005	≈ 0.03	0.005	0.07	0.12	0.03
α	1.6	_	_		1.4	1.5	1.5
β	1.8	2.5	0.2	0.8	1.8	-0.6	1.8

The parameters were estimated from Haar fluctuation structure functions using the relations $H = \xi(1)$, $H - C_1 = \xi'(1)$, $\alpha = \xi''(1)/C_1$; see the discussion in Sect. 4. Note that the approximation $\beta = 1 + 2H$ is accurate to $\approx 2C_1$

[a,b] The exponents in the weather and macroweather regimes are from a variety of sources reviewed in Lovejoy and Schertzer (2013). The local and global scale weather exponents are given using the 20CR data at hourly resolution. The local value H ≈ −0.4 is for land, H ≈ −0.2 for ocean, the global value (≈−0.2) being dominated by ocean. The global macroweather exponent is from Fig. 4a, the 20CR. The α value was not estimated since the intermittency was too small. We could also mention that the transition from macroweather to climate is a little different in the industrial and pre-industrial epochs, the former being a little smaller 10–30 years, see Lovejoy et al. (2013a)

[c] The climate exponents were estimated from Epica and Vostok ice core paleotemperatures

[d] The macroclimate exponents were estimated from Epica ice core and Huybers benthic ocean cores

[e] The megaclimate exponents were estimated from The Veizer and Zachos benthic cores

there was no implication that the underlying processes might have nontrivial scaling over any significant range. In contrast, scaling symmetries, were explicitly invoked to justify the alternative composite picture (Lovejoy and Schertzer 1984, 1986] which profited from early ocean and ice core paleotemperatures and used both spectra and (real space) structure function statistical analyses. These analyses already clarified the following points: (a) the distinction between the variability of regional and global scale temperatures with at least the local temperatures having a high frequency scaling regime with $\beta \approx 1.8$ (down to $\approx(1 \text{ month})^{-1}$), (b) this is followed by a fairly flat lower frequency relatively flat "spectral plateau" down to $\approx(400 \text{ yrs})^{-1}$ for local temperatures (but only to $\approx(5 \text{ yrs})^{-1}$ for global temperatures), (c) that at frequencies below the plateau below that there was a another scaling range down to frequencies of the order of $\approx(50 \text{ kyrs})^{-1}$ with an exponent $\beta \approx 1.8$, (d) that the latter scaling regime could quantitatively explain the magnitudes of the temperature swings between interglacials ("ice ages"): the "interglacial window" (see below).

We have mentioned that this picture has been supported by other scaling composites (Shackleton and Imbrie 1990; Pelletier 1998; Huybers and Curry 2006) but even without producing composites, other authors shared the scaling framework, e.g. (Koscielny-Bunde et al. 1998; Talkner and Weber 2000; Ashkenazy et al. 2003; Bunde et al. 2005; Rybski et al. 2008; Franzke 2010; Lennartz and Bunde 2009; Franzke et al. 2013; Rypdal and Rypdal 2014). Their results are qualitatively very similar—including the positions of the scale breaks; the main innovations are (a) the increased precision on the β estimates and (b) the basic distinction between continental and oceanic spectra including their exponents. We could also mention the composite of (Fraedrich et al. 2009) which is a modest adaptation of Mitchell's: it innovates by introducing a single scaling regime from ≈3 to ≈100 years.

Using real temperature and paleotemperature data, examples showing the behaviours of the different regimes are graphically illustrated Fig. 1e where the resolutions have been chosen as much as possible in order to show series with behaviours mostly from single regimes. To make the comparisons more objective, they have been nondimensionalized in time (each using 180 resolution units overall) and by normalizing them by their overall ranges (from bottom to top the series resolutions were 1 h, 1 month, 400 yrs, 14 kyrs, 370 kyrs and 1.23 Myrs). Notice that in the weather regime (Fig. 1e, bottom, and bottom right of Fig. 1d) the temperature seems to "wander" up or down like a drunkard's walk so that temperature differences typically increase over longer and longer periods. Turning to the macroweather series (Fig. 1e, second from the bottom and in Fig. 1d, the 16 day resolution, 34.5 years long series), we see that it has a totally different appearance with successive fluctuations on the contrary tending to cancel each other out, i.e. with decreases followed by partially cancelling increases (and visa versa). At first sight, this vindicates the "climate is what you expect" idea since averages over longer and longer periods will clearly converge. From this, we anticipate that at decadal—or certainly at centennial scales—that we will see at most smooth, slow variations. However, when we turn to the century resolution climate series (Fig. 1e, third from the bottom) on the contrary, we once again see weather-like wandering. The top two series in Fig. 1e takes this observation to even longer time scales showing that this pattern of cancelling

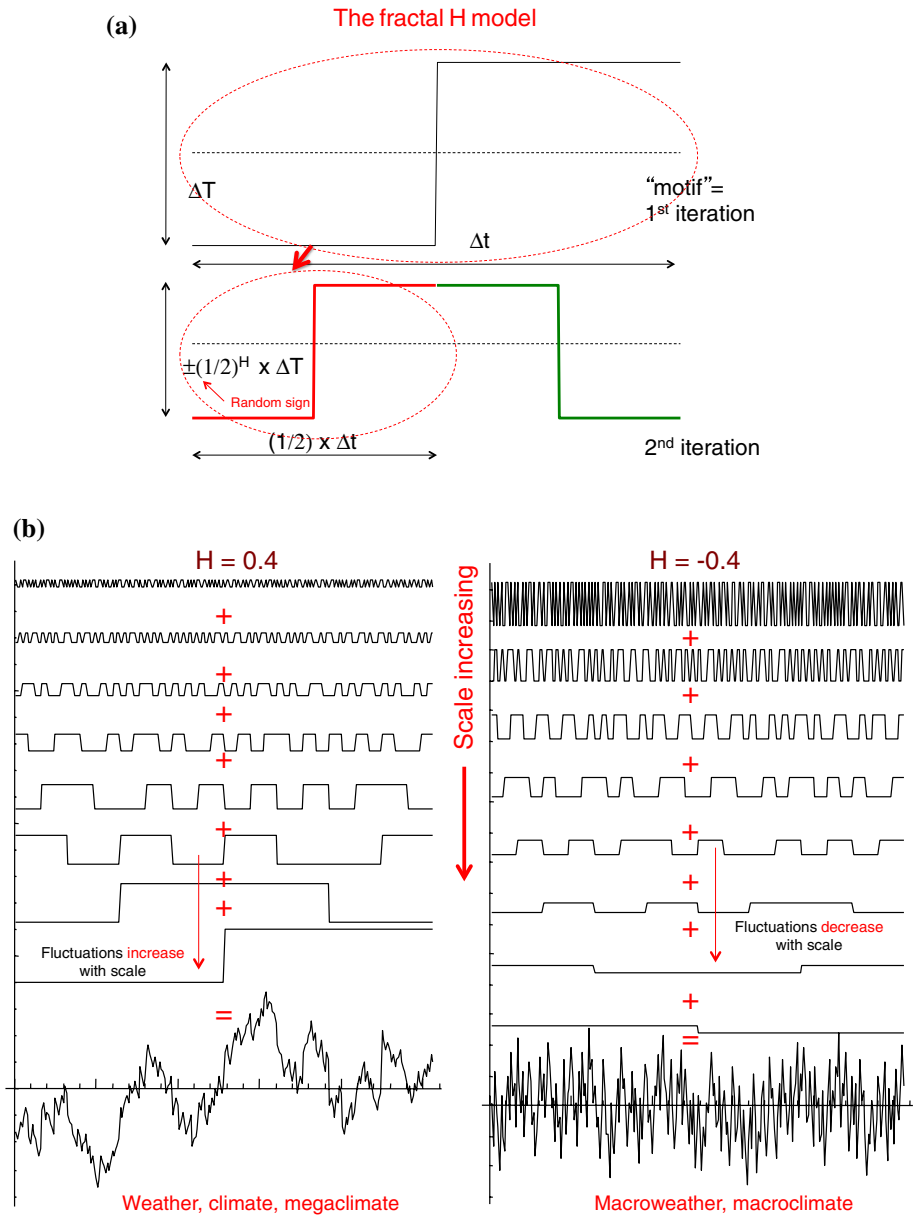

Fig. 3 **a** The first two steps in the construction of the fractal H model. To obtain the second row, the motif (i.e. a basic "fluctuation", *top row*) is reduced by a factor 2 in the horizontal and by 2^H in the *vertical* and then multiplied by a random sign, this is placed in the left hand half of the figure; the right hand half has the same shape but with another random sign. **b** The first 8 steps in the construction of the fractal H model with the sum, bottom series. In the left hand column we show the result for $H > 0$, the right, $H < 0$. In the $H > 0$ case we see that the amplitude of the fluctuations decreases as we go to smaller scales whereas in the $H < 0$ case, they increase

and wandering repeats once more (see Table 2, Sect. 5.3 where we also discuss the interpretation of these benthic $\delta^{18}O$ series).

Below we shall see that the fluctuations $\Delta T(\Delta t)$ over a time interval Δt (defined precisely in Sect. 4) are in each case roughly scaling (power laws) of the form $\Delta T(\Delta t) \approx \Delta t^H$ so that the sign of H qualitatively distinguishes the "wandering" ($H > 0$) or "cancelling" ($H < 0$) behaviours (since $\beta \approx 2H + 1$, the critical value $H = 0$ roughly corresponds to a critical spectral exponent $\beta = 1$). H is the "fluctuation exponent" (also called the "nonconservation" exponent) that we discuss in more detail in Sect. 4. It is denoted "H" in honour of Edwin Hurst but in general—unless the process is Gaussian—it is not the same as the Hurst (i.e. "R/S") exponent (e.g. for a standard random walk (Brownian motion) they both yield $H = ½$). In nonlinear dynamical systems, power laws arise when over a range of scales there are no processes strong enough to break the scaling symmetry. Another way of putting this is to say that the dominant dynamical processes occur in synergy over a wide range of scales, with the resulting behaviour displaying no characteristic size or duration. We can express this in yet another way in terms of systems theory: $H < 0$ indicates negative feedbacks occurring over a wide range of scales in a scale invariant way whereas $H > 0$, indicates positive feedbacks occurring over a wide range (this should not be confused with persistence and antipersistence which for Gaussian processes refer to fluctuations growing more or less quickly than Brownian motion).

In order to understand this H exponent, consider the simple (essentially pedagogical) fractal construction shown in Fig. 3a, b, that—for want of a better name—we call the "H model" (when $1 > H > 0$ it is a variant on the "pulse in pulse" model, and has divergence of statistical moments of order $> 1/H$, i.e. $\langle \Delta T^q \rangle \rightarrow \infty$ for $q > 1/H$, see Lovejoy and Mandelbrot 1985). To simulate a series with fluctuation exponent H over the unit interval, start with the basic fluctuation, the step function labelled "motif" in Fig. 3a (top); the dashed line indicates the horizontal axis so that the left half is negative, the right half is (symmetrically) positive. To obtain the 2nd generation of the construction, compress the motif by a factor two in the horizontal and 2^{-H} in the vertical and place the result in the left half of the interval, then multiply it by a random sign. Finally, repeat with another random sign and place the result in the right half interval. The figure shows the result for signs $+$, $-$; this defines the fluctuations at the corresponding reduced scale. Figure 3b shows the result when this is iterated 8 times; the left column with $H > 0$, the right column, $H < 0$. The final fractal process is obtained by summing all the contributions. Notice that in the $H > 0$ process, the fluctuations decrease with scale so that the process is dominated by the larger scales, conversely for the $H < 0$ process. When H < 1 the process has mean fluctuations $\langle \Delta T(\Delta t) \rangle \propto \Delta t^H$.

3 Scaling in the weather, macroweather and climate regimes

In this section, we review and discuss the three high frequency regimes whose scaling is relatively well established and quantified, we postpone discussion of the much less studied low frequency macroclimate and megaclimate regimes until Sect. 5.3.

Taken individually, for the weather ($\Delta t \approx < \tau_w$; $\tau_w \approx 10$ days), macroweather ($\tau_w < \Delta t < \tau_c$; preindustrial epoch: $\tau_c \approx 50$–100 yrs, industrial epoch, $\tau_c \approx 10$–30 yrs), and climate ($\Delta t > \tau_c$) regime, there are now many studies supporting the scaling picture and estimating various scaling exponents in each. Starting with the climate regime, numerous paleo temperature series (mostly from ice and ocean cores) have been analyzed and there is broad agreement on their scaling nature with spectral exponents estimated in the range $\beta_c \approx 1.3$ to 2.1 over the range from hundreds to tens of thousands of years, (Lovejoy and Schertzer 1986, 2012a; Schmitt et al. 1995; Ditlevsen et al. 1996; Pelletier 1998; Ashkenazy et al. 2003; Wunsch 2003; Huybers and Curry 2006; Blender et al. 2006; Lovejoy 2013; Rypdal and Rypdal 2014). These analyses employed diverse techniques including spectra, difference and Haar structure functions as well as Detrended Fluctuation Analysis so that the results are fairly robust. In addition, as discussed below (Fig. 4a–e), further analyses from surface temperatures, multiproxy reconstructions and 138 year long Twentieth Century reanalysis (20CR, Compo et al. 2011), lend this further quantitative support.

Similarly, in the macroweather regime, there are now many studies finding scaling with spectral exponents $\beta_{mw} < 1$, e.g. for the temperature; with some variation in β_{mw} between oceans and continents, northern latitudes and tropics: (Lovejoy and Schertzer 1986; Pelletier 1998; Huybers and Curry 2006; Fraedrich and Blender 2003; Koscielny-Bunde et al. 1998; Bunde et al. 2004; Eichner et al. 2003; Lennartz and Bunde 2009; Blender et al. 2006; Fraedrich et al. 2009; Lanfredi et al. 2009). Since β_{mw} is small, log–log spectra appear as fairly flat hence the original term "spectral plateau". A review of the ubiquitous empirical evidence for this include analyses of the temperature, wind, humidity, geopotential height, rain, vertical wind, and the North Atlantic Oscillation, Southern Oscillation and Pacific Decadal Oscillation indices (Lovejoy and Schertzer 2010, 2013).

Of the three high frequency regimes, the only one where the idea of an at least roughly scaling spectrum is still somewhat controversial is the weather regime (scales $< \tau_w \approx 10$ days). To understand the debate, recall that the classical turbulence theories describing the statistical variability of weather are all based on isotropic scaling, the most famous being the Kolmogorov $k^{-5/3}$ spectrum for the wind (k is a wavenumber). However, the strong vertical atmospheric stratification prevents isotropic scaling from holding over any scale ranges spanning the scale thickness of the atmosphere ($\approx$10 km). At larger scales, one must therefore abandon either the scaling or the isotropy assumption. Influenced by Van der Hoven's meso-scale gap (Sect. 1), and following Kraichnan's development of 2-D turbulence and Charney's extension to (still essentially 2D) "quasi geostrophic" turbulence, the usual choice was to retain isotropy and to divide the dynamics into 2D isotropic (large scale) and 3D isotropic (small) scale regimes (Kraichnan 1967; Charney 1971). However, starting with (Schertzer and Lovejoy 1985), a growing body of evidence and theory has supported the alterative anisotropic scaling hypothesis. Thanks both to modern empirical evidence (e.g. the review Lovejoy and Schertzer 2010, 2013) and a recent massive aircraft study (Pinel et al. 2012), but also to theoretical arguments showing that the governing equations are symmetric with respect to anisotropic scaling symmetries (Schertzer et al. 2012), the question increasingly has been settled in favor of anisotropic scaling (see the recent debate Lovejoy et al. 2009, 2010; Lindborg et al. 2010a, b; Schertzer et al. 2011, 2012; Yano 2009). The implications of this anisotropic spatial scaling for the temporal statistics are discussed in Radkevitch et al. (2008), Lovejoy and Schertzer (2010) and Pinel et al. (2014).

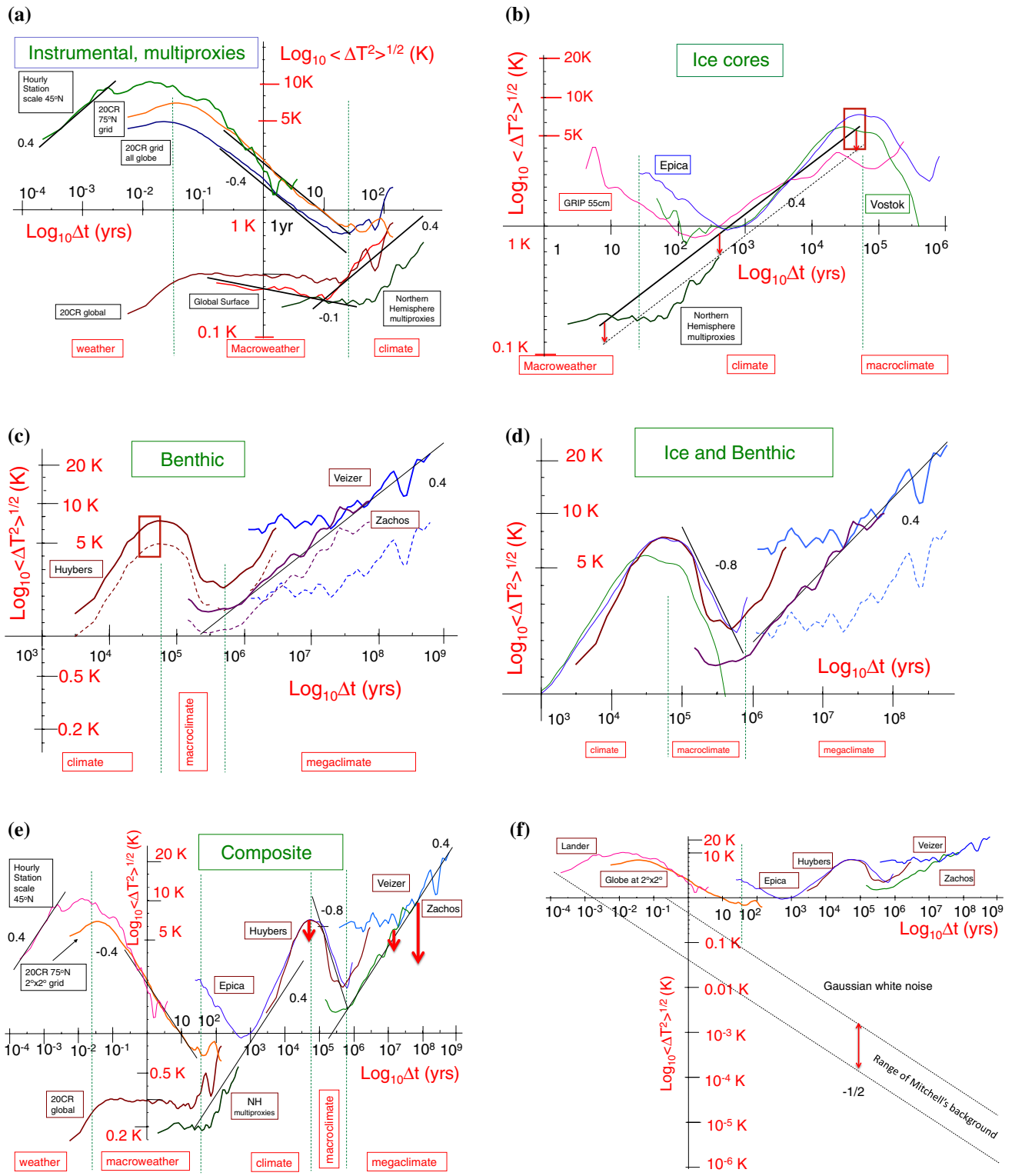

A review of diverse evidence from reanalyses, in situ and remotely sensed data (Lovejoy and Schertzer 2010, 2013) shows that for wind, temperature, humidity, pressure, short and long wave radiances, β_w is commonly in the range 1.5–2 (certainly > 1, hence $H > 0$). The existence of a basic transition in the range ≈5 to 20 days has been recognized at least since (Van der Hoven 1957) who noted a low frequency spectral "bump" at around 5 days. Later, the corresponding features in the temperature and pressure spectra were termed "synoptic maxima" by Kolesnikov and

◀**Fig. 4** **a** Empirical RMS temperature fluctuations ($S(\Delta t)$), local and global scale analyses of instrumentally based temperatures. The *upper left curve* (*green*) is from hourly station data (Lander Wyoming, USA) from 2005 to 2008 (4 years) it has been detrended daily and annually. The *two curves* below it (*orange*, *blue*) are at grid point scale (2° × 2°) daily scale fluctuations averaged over 75°N, and over the whole globe respectively from the 20CR, 700 mb. Also shown are lines with reference slopes $\xi(2)/2 = 0.4, -0.4 \approx H$. Below these, the same data averaged globally and then analysed in time (*brown*); the variability is much lower due to the global spatial averaging. The *curve* below that (*red*) is the result from averaging monthly resolution temperature series (NOAA NCDC, NASA GISS, HadCRUT3) and below this, the average of three post 2003 multiproxy structure functions from 1500 to 1900 (pre-industrial; Huang 2004; Ljungqvist 2010; Moberg et al. 2005). The slight difference (of about $10^{0.1}$) between this surface curve and the 20CR global curve is because for technical reasons, the 20CR data were at the 700 mb level. The instrument (*red*) and multiproxy (*green*) structure functions show transitions from $H < 0$ to $H > 0$ at somewhat different time scales, this is because in the industrial epoch, the anthropogenic forcing is stronger than the natural forcing. The *dashed green lines* indicate the rough transition times where the slopes change sign indicating that the behaviour changes from fluctuations increasing and decreasing with scale: weather, macroweather to climate. The *bottom five curves* are from (Lovejoy and Schertzer 2012a). **b** Using the same scale as in (**a**), we compare the RMS Haar temperature fluctuations for the Greenland GRIP core at 55 cm (magenta; the same core as in Fig. 1b but at lower resolution and going back to 248 kyrs, see Table 1), the Vostok and EPICA Antarctic cores (*green, blue* respectively based on Deuterium). The Vostok core goes back 420 kyrs, for Epica, see Fig. 1b and "Appendix"). Also shown is the interglacial "window" corresponding to glacial-interglacial transitions of ±2 to ±4 K (i.e. $S(\Delta t) = 4, 8$ K) over half periods 30–50 kyrs. Also for reference are the pre-industrial multiproxies from (**a**). The three ice core paleo series had nonuniform resolutions but were analysed without interpolation using a new Haar fluctuation algorithm. *Solid* and *dashed reference lines* with slopes $\xi(2)/2 = 0.4$ are shown corresponding to a spectral exponent $\beta = 1 + \xi(2) = 1.8$, a *flat curve* in the above corresponds to $\beta = 1$. These can be compared with the Haar fluctuation analyses of the Vostok and GRIP cores using interpolated series (see Lovejoy and Schertzer 2012a). The *dashed line* has been shifted downwards by a factor 1.5 to indicate the approximate effect of high latitude amplification. **c** Analysis of the three benthic paleo series from Fig. 1a, 2a, b analysed without interpolation. The *solid red* and *purple lines* show the structure functions for Huybers and Zachos that were converted to temperature using the calibration −6.5 K/δ^{18}O, roughly 50 % larger than canonical −4.5 K/δ^{18}O (shown as *dashed*) this roughly takes into account the high latitude amplification (see Table 1 for information on the data, see Sect. 5.3 for a discussion of the calibration). As can be seen in (**d**), the calibration of −6.5 K/δ^{18}O gives much better agreement with our knowledge of glacial-interglacial variations. For the Veizer data, the *solid blue* indicates −4.5 K/δ^{18}O, the *dashed blue* −1.5 K/δ^{18}O is an extreme limit potentially appropriate to tropical oceans. A reference line with slope $\xi(2)/2 = 0.4$ is shown corresponding to a spectral exponent $\beta = 1 + \xi(2) = 1.8$. The proposed low frequency regimes: climate, macroclimate and megaclimate, are separated by *dashed green lines* at roughly 80 kyrs, 500 kyrs. **d** A composite focusing on the macroclimate and megacimate regions, using part of the antarctica ice core analyses (only the part $\Delta t > 1$ kyr is shown, *Vostok dark green*, Epica, *thin blue*, *left*) with the benthic series (*purple*, Zachos, *brown* Huybers with −6.5 *K*/δ^{18}O). The Veizer series uses −4.5 *K*/δ^{18}O (*solid blue*) and −1.5 *K*/δ^{18}O (*dashed blue*). The reference *lines* have the slopes indicated. All the proxies agree quite well for $\Delta t \approx$ <200 kyrs and for $\Delta t \approx >$ 20 Myrs and the Epica macroclimate regime has quite linear log–log regime close to the reference line (slope −0.8). **e** This is a wide scale range composite series from the previous analyses (**a**–**c**), showing atmospheric variability over the range from 1 h to 553 million years. In order to avoid cluttering the diagram, only representative *curves* have been shown (notably with −6.5 *K*/δ^{18}O for Huybers and Zachos, −4.5 *K*/δ^{18}O for Veizer). We also indicate the 5 regimes: weather, macroweather, climate, macroclimate and megaclimate. **f** The composite with a Gaussian white noise (slope −1/2) superposed. Following Mitchell (1976), the white noise "background" was assumed to start at 1 h, the amplitude given by the Lander Wyoming station data at hourly resolution. Mitchell's spectral background (Fig. 2a) ranged over about two orders of magnitude corresponding to one order of magnitude in RMS fluctuations, his entire range of background is roughly between the two *dashed black lines*

Monin (1965) and Panofsky (1969). More recently, in the same spirit as Mitchell, the transition has been modeled (e.g. AchutaRao and Sperber 2006) as an Orenstein-Uhlenbeck process i.e. with $\beta_w = 2$, $\beta_{mw} = 0$, corresponding to $H_w = 1/2$, $H_{mw} = -1/2$, although this is not a very accurate approximation and can be misleading (Stolle 2012). Finally, (Vallis 2010) proposed a (nonscaling) mechanism by suggesting that τ_w is determined by the lifetimes of baroclinic instabilities. These were estimating by the inverse Eady growth rate (τ_{Eady}) and yields $\tau_w \approx \tau_{Eady} \approx 4$ days. However this result requires a linearization of the equations about a hypothetical state having uniform shear and uniform stratification across the entire troposphere. In comparison, the real troposphere has highly nonuniform shears and stratifications, its variability is so strong that it is characterized by anomalous scaling exponents throughout (Lovejoy et al. 2007) (including $H \approx 0.75$ for the horizontal wind in the vertical direction). Another difficulty with using $\tau_w \approx \tau_{Eady}$ is that τ_{Eady} is inversely proportional to the Coriolis parameter so that it diverges at the equator whereas the empirical τ_w is not very sensitive to latitude.

Indeed, a seductive feature of the (anisotropic) scaling framework is that it fairly accurately predicts the weather to macroweather transition scale $\tau_w \approx 10$ days. The argument is as follows: the sun provides ≈240 W/m^2 of heating with a 3 % efficiency of conversion to kinetic energy (see Monin 1972). The energy is distributed reasonably uniformly over the troposphere, leading to a turbulent energy flux density (ε) close to the observed global value $\varepsilon \approx 10^{-3}$ W/kg (Lovejoy and Schertzer 2010); this is the flux of energy from large to small scales. The model predicts that this turbulent energy flux is the fundamental driver of the horizontal dynamics and thus that planetary structures have eddy-turnover times of $\approx \varepsilon^{-1/3} L_e^{2/3} \approx 10$ days where $L_e = 20000$ km is the largest great circle distance on the earth. The analogous calculation for the ocean using the empirical (near surface) ocean turbulent flux $\varepsilon \approx 10^{-8}$ W/kg, yields a lifetime of ≈1 year which is indeed the scale

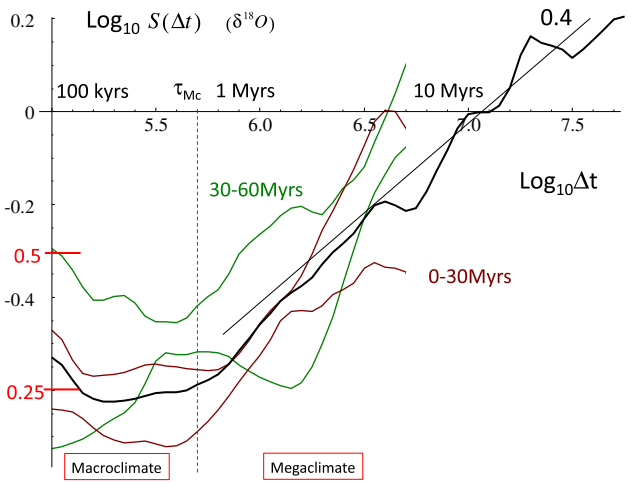

Fig. 5 The RMS Haar fluctuations of the Zachos $\delta^{18}O$ series analysed over 6 successive 10 Myr segments, using the no interpolation algorithm ("Appendix"). The number of data points in each segment decreases quickly with age, in successive 10 Myr sections there were: 6,449, 2,850, 3,250, 1,300, 565, 310 measurements. The *brown curves* are the one standard deviation limits estimated from the first 3 segments (corresponding roughly to the early Oligocene), the period when ice caps contained significant volumes of ice. The *green curves* are for the corresponding limits for the next 30 Myr period, the *black curve* is the mean for the entire data set. We see that the *error bars* of the first and second 30 Myr segments fairly consistently overlap indicating that they are reasonably compatible with the hypothesis of being produced by the same stochastic process. Also shown is the macroclimate-megaclimate transition time (0.5 Myrs) and the reference line slope 0.4 indicating the overall scaling

separating a high frequency "ocean weather" (with $\beta > 1$) from a low frequency "macro-ocean weather" with $\beta < 1$ (Lovejoy and Schertzer 2012a; at depth, ε is much lower and the corresponding lifetimes are much longer). The same reasoning predicts the critical weather/macroweather transition on Mars to be $\approx$1.5 days, this has been confirmed with Mars lander and reanalysis data (Lovejoy et al. 2014b).

This picture allows us to understand the weather/macroweather transition since it validates the use of the stochastic turbulence based Fractionally Integrated Flux model (FIF, i.e. cascades Schertzer and Lovejoy 1987). The FIF model shows that whereas in the weather regime, fluctuations depend on interactions in both space and in time, at lower frequencies they become "quenched" so that only the temporal interactions are important and τ_w marks a "dimensional transition" (Lovejoy and Schertzer 2010). Physically, at scales $\Delta t < \tau_w$ the statistics depend on structures with lifetimes Δt; at scales $\Delta t > \tau_w$ they depend on the statistics of many planetary sized structures. In addition, GCM control runs (i.e. without climate forcings) and the basic FIF model fairly accurately reproduce the macroweather exponents (see below).

4 Real space fluctuations and analyses

In spite of the now burgeoning evidence that the atmosphere's natural variability is scaling over wide ranges, the approaches to understanding natural variability are still scale bound. Natural variability is largely identified with quasi-periodic behaviours which—when present—have the advantage of being predictable. Examples of proposed periodicities are El Nino Southern Oscillation (ENSO; 3–5 years) to multidecadal (e.g. Pacific Decadal Oscillation, Atlantic Multidecadal Oscillation) to millennial scales see (Delworth et al. 1993; Schlesinger and Ramankutty 1994; Mann and Park 1994; Mann et al. 1995, 2014; Bond et al. 1997; Isono et al. 2009). An additional reason for a focus on quasi-periodic behaviour is that whereas spectra are ideal for understanding periodic processes, they are not optimal for scaling processes. For these, the corresponding real space analyses are more straightforward to interpret; this is particularly true when comparing spectra from different data types with different resolutions. In this section we show how this works.

In Sect. 2, in order to understand the qualitatively different behaviours in Fig. 1a–e, associated with the fluctuation exponent H, we introduced the H model. More generally in a scaling regime, $\Delta T = \varphi\, \Delta t^H$ where φ is a controlling dynamical variable (e.g. a dynamical flux) whose mean $<\varphi>$ is independent of the lag Δt (i.e. independent of the time scale). The behavior of the mean fluctuation is thus $< \Delta T > \approx \Delta t^H$ so that if $H > 0$, on average fluctuations tend to grow with scale whereas if $H < 0$, they tend to decrease. Note that the mean is the first order moment; moments of other orders (i.e. $< \varphi^q >$ for $q \neq 1$) will generally depend on Δt, this is associated with multifractal behaviour (see below).

Although it is traditional (and often sufficient) to define fluctuations by absolute differences $\Delta T(\Delta t) = |T(t + \Delta t) - T(t)|$, for our purposes this is *not* sufficient. Instead we should use the absolute difference of the mean between t and $t + \Delta t/2$ and between $t + \Delta t/2$ and $t + \Delta t$. Technically, the latter corresponds to defining fluctuations using Haar wavelets rather than "poor man's" wavelets (differences). While the latter is adequate for fluctuations increasing with scale (i.e. $H > 0$), mean absolute differences generally increase and so when $H < 0$, they do not correctly estimate fluctuations. The Haar fluctuation (which is useful for $-1 < H < 1$) is particularly easy to understand since (with proper "calibration") in regions where $H > 0$, it can be made very close to the difference fluctuation and in regions where $H < 0$, it can be made close to another simple to interpret "anomaly fluctuation" (the original term "tendency fluctuation" is less intuitive, Lovejoy and Schertzer 2012b). While other techniques such as Detrended Fluctuation Analysis (Peng et al. 1994;

Kantelhardt et al. 2002; Monetti et al. 2003) perform just as well for determining exponents, they have the disadvantage that their fluctuations are not at all easy to interpret (they are the standard deviations of the residues of polynomial regressions on the running sum of the original series; see (Lovejoy and Schertzer 2012b).

Once estimated, the variation of the fluctuations with scale can be quantified by using their statistics; the qth order structure function $S_q(\Delta t)$ is particularly convenient:

$$S_q(\Delta t) = \left\langle \Delta T(\Delta t)^q \right\rangle \tag{1}$$

where "<.>" indicates ensemble averaging. In a scaling regime, $S_q(\Delta t)$ is a power law

$$S_q(\Delta t) = \left\langle \varphi^q_{\Delta t} \right\rangle \Delta t^{qH} \propto \Delta t^{\xi(q)}; \quad \left\langle \varphi^q_{\Delta t} \right\rangle \propto \Delta t^{K(q)}; \quad \xi(q) = qH - K(q) \tag{2}$$

where the exponent $\xi(q)$ has a linear part qH and a convex (generally nonlinear) part $K(q)$ and since $<\varphi> =$ constant, $K(1) = 0$. Since Gaussian processes have $K(q) = 0$, $K(q)$ characterizes the strong non Gaussian, multifractal variability; the "intermittency". In the macroweather regime $K(2)$ is typically small ($\approx$0.01–0.03, see Table 2), so that the RMS variation $S_2(\Delta t)^{1/2}$ (denoted simply $S(\Delta t)$ below) has the exponent $\xi(2)/2 = H - K(2)/2 \approx H = \xi(1)$. In the climate, macroclimate and megaclimate regimes, this intermittency correction is a bit larger (see Table 1 and caption). Note that since the spectrum is a second order statistic, we have the useful relationship $\beta = 1 + \xi(2) = 1 + 2H–K(2)$. When $K(2)$ is small, $\beta \approx 1 + 2H$ so that as mentioned earlier, $H > 0$, $H < 0$ corresponds to $\beta > 1$, $\beta < 1$ respectively.

Using universal multifractals (Schertzer and Lovejoy 1987) the function K(q) can be characterized by two parameters C_1, α. These can be estimated using the relations $H = \xi(1)$, $H - C_1 = \xi'(1)$, $\alpha = \xi''(1)/C_1$ (see Table 2). The C_1, α, parameters characterize the intermittency near the mean ($q = 1$) and the curvature near the mean respectively; for universal multifractals the latter is the equal to the Levy index of the generator of the process, for these, $K(q) = C_1(q^\alpha - q)/(\alpha - 1)$ (see Eq. 2). Note that for universal multifractals, we therefore have $\xi(2)/2 = H - A_\alpha C_1$ where $A_\alpha = (2^{\alpha-1} - 1)/(\alpha - 1)$ and for $2 < \alpha < 1.4$ (the range relevant here), we find $1 > A_\alpha > 0.8$ hence the difference between the exponent of the mean and RMS fluctuations is: $\xi(1)–\xi(2)/2 = A_\alpha C_1 \approx C_1$. Also, since the spectral slope $\beta = 1 + \xi$ (2) we see that the approximation $\beta = 1 + 2H$ is accurate to $\approx 2C_1$.

When $S(\Delta t)$ is estimated for various in situ, reanalysis, multiproxy and paleo temperatures, one obtains Fig. 4a–e. The key points to note are:

a. the five qualitatively different regimes corresponding to weather, macroweather climate, macroclimate, megaclimate with $S(\Delta t)$ alternately increasing and decreasing with scale ($H_w > 0$, $H_{mw} < 0$, $H_c > 0$, $H_{mc} < 0$, $H_{Mc} > 0$, see Table 2). The weather, and climate transitions are at $\tau_w \approx$ 5–10 days and $\tau_c \approx$ 50–100 yrs (Fig. 4a, b) note that in the industrial period τ_c is a bit lower ($\approx$10–30 yrs)—in Fig. 4a see the 1880–2008 surface series and compare its S(Δt) with those of the preindustrial multiproxies that have $\tau_c \approx$50–100 yrs. This difference is because over the last century, anthropogenic forcing has become dominant for scales greater than about 10–30 yrs. If the anthropogenic part of the temperatures since 1880 are estimated using the log CO_2 concentration as a surrogate for all anthropogenic effects, then the industrial and pre-industrial fluctuation statistics are identical to within measurement uncertainties, see (Lovejoy 2014b). Moving to longer time scales, there is evidence for a macroclimate regime at scales $>\tau_{mc} \approx$ 80 kyrs and a megaclimate regime at scales longer than $\tau_{Mc} \approx$ 0.5 Myr, see Figs. 4c–e, 5. Notice that the transition times are close to—but not identical with—those inferred from the spectral breaks in Fig. 2a, b. Small differences are not surprising because the correspondence between real and Fourier space scaling is strictly only valid for wide enough ranges of scale.
b. The difference between the local and global fluctuations.
c. the "glacial/interglacial window" corresponding to overall ±2 to ±4 K variations (i.e. $S(\Delta t) \approx 4$, 8 K, due to "polar amplification" it is roughly 50 % larger than the global variation; the S(Δt) corrected for this is shown in Fig. 4c (see also Figs. 2a, b, 4b), over scales with half periods of 30–50 kyrs; the curve must pass through the window in order to explain the glacial/interglacial transitions. Starting at 10–30 yrs, one can plausibly extrapolate the global surface and 20CR 700 *mb* $S(\Delta t)$'s using $H = 0.4$ ($\beta \approx 1.8$, Fig. 4b), all the way to the interglacial window (with nearly an identical S as in Lovejoy and Schertzer (1986)). Similarly, the local temperatures and multiproxies also seem to follow the same exponent with slightly different τ_c's and seem to extrapolate respectively a little above and below the window. (At high laltitudes, the 20CR surface temperatures have errors (G. Compo private communication); the 700 mb temperatures were used because they were more globally reliable).
d. Gaussian white noise (close to Mitchell's "background" spectrum) yields $H = -1/2$; this is shown in Fig. 4f which makes it abundantly clear that the background must be very far from a white noise.

An important advantage of Haar fluctuations is that due to the temporal averaging (recall they combine averaging

and differencing), they are insensitive to the resolutions of the series (they give identical statistics independently of the series resolutions). This is very useful since—with the exception of the (instrumental) high frequency weather and macroweather data—the paleo data typically has highly variable temporal resolution, hence the need for the new technique for estimating Haar fluctuations discussed in "Appendix".

We should note that throughout, we have simply used the recommended paleo calibrations which are all linear. Since our estimates of H are independent of a linear transformation, we would obtain identical H estimates had the raw (e.g., $\delta^{18}O$) data been used. More specifically, adding a constant makes no difference since the Haar fluctuation only depends on differences and changing a multiplicative calibration constant will simply change the fluctuation amplitudes, hence result in an up/down shift on a log–log plot. By comparing different series and considering the amplitude of their fluctuations, a consistent set of multiplicative calibration constants can easily be obtained.

Fluctuation statistics may seem arcane but their physical interpretation is pretty straightforward. For example, in the weather regime, larger and larger fluctuations "live" for longer and longer "eddy turnover" times. At any given time scale, the fluctuations are dominated by structures with corresponding spatial scales and this relationship holds up to structures of planetary scales with lifetimes $\approx$10 days. For periods longer than this, the statistics are dominated by averages of many planetary scale structures, and these fluctuations tend to cancel out: for example large temperature increases are typically followed (and partially cancelled) by corresponding decreases. The consequence is that in this macroweather regime, the average fluctuations diminish as the time scale increases. At some point—at around 50–100 years depending on geographic location and time (and as little as 10–30 years in the recent period when anthropogenic variability is important), these weaker and weaker fluctuations—whose origin is in weather dynamics—become dominated by increasingly strong lower frequency climate processes. These not only include changing external solar, volcanic orbital or anthropogenic "forcings"—but quite likely also new and increasingly strong slow (internal) climate processes—or by a combination of the two: forcings with feedbacks. A relevant example of a slow dynamical process that is not currently fully incorporated into GCM's is land-ice dynamics although there are many slow biogeochemical processes that might also be relevant. The overall effect is that in the resulting climate regime, fluctuations tend to grow again with scale in an "unstable" manner, very similar to the way they grow in the weather regime.

5 Discussion

5.1 The Climate is not what you expect

In his monumental "Climate: Past, Present, and Future" Horace Lamb argued that the early scientific view was "climate as constant" (Lamb 1972). Reflecting this, in 1935 the International Meteorological Organization adopted 1901–1930 as the "climatic normal period". Following the post war cooling, this view evolved: for example the official American Meteorological Society glossary (Huschke 1959) defined the climate as "the synthesis of the weather" and then "…the climate of a specified area is represented by the statistical collective of its weather conditions during a specified interval of time (usually several decades)". Although this new definition in principle allows for climate change, the period 1931–1960 soon became the new "normal", the ad hoc 30 year duration became entrenched, today 1961–1990 is commonly used. Mindful of the extremes, Lamb warned against reducing the climate to just "average weather", while viewing the climate as "…the sum total of the weather experienced at a place in the course of the year and over the years", (Lamb 1972).

Lamb's essentially modern view allows for the possibility of climate change and is closely captured by the popular expression: "The climate is what you expect, the weather is what you get" (the character Lazurus Long in Heinlein (1973), but often attributed to Mark Twain). It is also close to the US National Academy of Science definition: "Climate is conventionally defined as the long-term statistics of the weather…" (Committee on Radiative Forcing Effects on Climate 2005) which improves on the "the climate is what you expect" idea only a little by proposing: "…to expand the definition of climate to encompass the oceanic and terrestrial spheres as well as chemical components of the atmosphere".

The Twain/Heinlein expression was strongly endorsed by the late E. Lorenz who stated: "Before embarking on a search for an ideal definition (of climate) assuming one exists, let me express my conviction that such a definition, when found must agree in spirit with the statement, "climate is what you expect"." (Lorenz 1995). He then proposed several definitions based on dynamical systems theory and strange attractors (see also Palmer 2005).

A variant on this, motivated by GCM modeling, was proposed by (Bryson 1997) (criticized by Pielke 1998): "Climate is the thermodynamic/hydrodynamic status of the global boundary conditions that determine the concurrent array of weather patterns." He explains that whereas "weather forecasting is usually treated as an *initial value* problem … climatology deals primarily with a *boundary condition* problem and the patterns and climate devolving

there from". This definition could be paraphrased "for given boundary conditions, the climate is what you expect". This and similar views provide the underpinnings for much of current climate prediction, including the recent idea of "seamless forecasting" (e.g. Palmer et al. 2008; Palmer 2012) in which seasonal scale model validation is applied to climate scale predictions (for a recent discussion, see Pielke 2012).

There are two basic problems with the Twain/Heinlein dictum and its variants. The first is that they are based on an abstract weather—climate dichotomy, they are not informed by empirical evidence. The glaring question of how long is "long" is either decided subjectively or taken by fiat as the WMO's "normal" 30 year period. The second problem is that it assumes that the climate is nothing more than the long-term statistics of weather. If we accept the usual interpretation—that we "expect" averages—then the dictum means that averaging weather over long enough time periods converges to the climate. With regards to external forcings, one could argue that this notion could still implicitly include the atmospheric response i.e. with averages converging to slowly varying "responses". However, it implausibly excludes the appearance of any new "slow", internal climate processes leading to fluctuations growing rather than diminishing with scale.

To overcome this objection, one might adopt a more abstract interpretation of what we "expect". For example if the climate is defined as the probability distribution of weather states, then all we "expect" is a random sample. However even this works only inasmuch as it is possible to merge fast weather processes with slow climate processes into a single process with a well defined probability distribution. While this may satisfy the theoretician, it is unlikely to impress the layman. This is particularly true since to be realistic we will see that one of the regimes in this composite model must have the property that fluctuations converge whereas in the other, they diverge with scale. To use the single term "climate" to encompass the two opposed regimes therefore seems at best unhelpful and at worst misleadling. The climate is therefore *not* what you expect: expect macroweather.

5.2 Implications for climate modelling, prediction, anthropogenic effects

Numerical weather models and reanalyses are qualitatively in good agreement with the weather/macroweather picture described above, although there are still some quantitative discrepancies in the values of the exponents, possibly due the hydrostatic approximation and numerical issues (Stolle et al. 2009; Lovejoy and Schertzer 2011). However, climate models (GCM's) are essentially weather models with various additional couplings (with ocean, carbon cycle, land-use, sea ice and other modelled processes). It is therefore not surprising that control runs (i.e. with no "climate forcings") generate macroweather (with $\beta_{mw} \approx 0.6$, $H_{mw} \approx -0.2$), and this apparently out to the extreme low frequency limit of the models [see the analyses and discussion in (Lovejoy et al. 2013a) as well as (Blender et al. 2006; Rybski et al. 2008), the same is true for control runs in simplified climate models, see (Lovejoy et al 2014a)]. Note that an important consequence of macroweather exponents in the range $-1/2$ to 0 is that they can be predicted with stochastic techniques, the forecast skill increases rapidly from zero ($H = -1/2$) as H tends to zero from below (work in progress).

> Avoiding anthropogenic effects by considering the pre-1900 epoch, for GCM climate models, the key question is whether solar, volcanic, orbital or other climate forcings are sufficient to arrest the $H < 0$ decline in macroweather fluctuations and to create an $H > 0$ regime with sufficiently strong centennial, millennial variability to account for the background variability out to glacial-interglacial scales. Analysis of several last millennium simulations has found that for the moment, their low frequency variabilities are too weak (Lovejoy et al. 2013a).

To understand this weak variability, one can examine the scale dependence of fluctuations in the radiative forcings (ΔR_F) of several solar and volcanic reconstructions; they are generally scaling with $\Delta R_F \approx A \Delta t^{H_R}$ (Lovejoy and Schertzer 2012c). If $H_R \approx H_T \approx 0.4$, then scale *independent* amplification/feedback mechanisms would suffice. However it was often found that $H_R \approx -0.3$ implying that the forcings become weaker with scale—even though the response grows with scale. This suggests the need to introduce new slow mechanisms of internal variability. Such mechanisms must have broad spectra; this suggests that their dynamics involve nonlinearly interacting spatial degrees of freedom such as the land-ice dynamics mentioned above.

Whatever the ultimate source of the growing fluctuations in the $H > 0$ climate regime, a careful and complete characterization of the scaling in space as well as in time (including possible space–time anisotropies) allows for new stochastic methods for predicting the climate. The idea is to exploit the particularly low variability of the averages at scale τ_c. Since $\tau_c \approx 30$ yrs—i.e. the conventional but ad hoc "climate normal" period—this not only justifies the normal but allows averages of relevant variables over it to define "climate states" and the changes at scales $\Delta t > \tau_c$ to define climate change (again, in the recent period, this defines the scale at which anthropogenic variability starts to dominate natural variability). Even without resolving the question of the dominant climate forcing and slow internal

feedbacks, one could use the statistical properties of the climate states—the system's "memory" implicit in the long range statistical correlations—combined with the growing data on past climate states in order to make stochastic climate forecasts (see below).

Another attractive application of this scaling picture is that by quantifying the natural variability as a function of space–time scales, it opens up the possibility of convincingly distinguish natural and anthropogenic variability. This is possible because the stochastic scaling framework allows one to statistically test specific hypotheses about the probability that the atmosphere would naturally behave in the way that is observed, i.e. to formulate rigorous statistical tests of any trends or events against the null hypothesis. Only if the probabilities are low enough should the hypothesis that the observed changes are natural in origin be rejected. Such estimates cannot be made using GCM's because we currently have little confidence in their centennial scale probability distributions; one must use empirical multiproxy distributions instead. For example, using CO_2 as a surrogate for all anthropogenic effects and taking into both long range statistical dependencies and extreme "fat tailed" probabilities, (Lovejoy 2014b) found that the probability of the global warming since 1880 being due to natural variability can be rejected with more than 99 % confidence. Similarly one can estimate the return periods for the postwar cooling and the current "pause" in the warming (Lovejoy 2014a). Work in progress applying this to global scale temperatures already shows that annual to decadal stochastic forecasts are comparable in accuracy to GCM's and adding spatial information (i.e. using space–time stochastic models) can only improve on this.

The scaling fluctuation approach thus allows quantitative (and hence convincing) answers to questions such as: how can the earth have prolonged periods of cooling in the midst of anthropogenic warming; or was this winter's record mild temperature really evidence for anthropogenic influence? Finally, the systematic comparison of model and natural variability in the preindustrial era is the best way to fully address the issue of "model uncertainty", to assess the extent by which the models are missing important slow processes.

5.3 Scaling at the longest scales: the Macroclimate and the megaclimate

5.3.1 The $\delta^{18}O$—temperature relation at Myr scales, latitudinal variations

Beyond the climate regime ($\Delta t > \tau_{mc} \approx 100$ kyrs, see Figs. 4c–e, 5) comparatively few statistical analyses have been made and the interpretation of the paleo data in terms of temperatures is also less clear: the situation is somewhat speculative. For example, although (Shackleton and Imbrie 1990) claimed that the log–log spectrum of benthic $\delta^{18}O$ was "approximately linear" from about 1 kyr to 100 Myr, it is possible that there are three different scaling regimes over this range of scales, not one. The other scaling interpretations of these very low frequencies are (Pelletier 1998; $\beta = 0$ i.e. white noise, in the macroclimate regime), and (Markonis and Koutsoyiannis 2013) who used the "climactogram" to characterize the scaling of the various series including the Veizer and Zachos series shown in Fig. 1a and analyzed in Figs. 4c–e, 5. However, as pointed out in Lovejoy et al. (2013b), the climactogram gives spurious exponents whenever $H > 0$, and this includes the climate ($\approx 10^2$–10^5 yrs) and the megaclimate regime at scales > 1 Myrs.

In the Huybers, Zachos and Veizer series, the $\delta^{18}O$ is from benthic organisms and varies both due to the temperature as well as the mean $\delta^{18}O$ of the water in which they lived. The basic relationship between $\delta^{18}O$ and temperature is an inverse one: increasing $\delta^{18}O$ is associated with decreasing temperatures although this relationship is complicated by the change in the $\delta^{18}O$ composition of the sea water due to the preferential sequestering of light sea water in ice caps. There are thus both direct and indirect links to the temperature via the ice sheets. For example (Veizer et al. 2000) has suggested that for the tropical oceans, that as much as 2/3 of the variation in $\delta^{18}O$ is due to the sequestering effect (close to the estimates of Zachos et al. (2001) for the early Oligocene, 33 Myrs to present). In addition, temperature variations are latitude dependent so that high latitude temperature variations are amplified by roughly 50 % above global variations. Although we essentially use the "canonical" calibration coefficient -4.5 $K/\delta^{18}O$ (Shaviv and Veizer 2003), and recommended by Barras et al. (2010) on the basis of laboratory experiments and near the earlier -4 $K/\delta^{18}O$ suggested by Shackleton and Imbrie (1990) for the last 70 Myrs), we have tried to take theses effects into account by various indications in Figs. 2a, b and 4b–e. For example, for the global (but largely tropical) Veizer series we have given not only the canonical -4.5 $K/\delta^{18}O$ calibration but also the limiting behaviour using the fairly extreme -1.5 $K/\delta^{18}O$ calibration as well. Also, the Zachos and Huyber series are mostly from high latitudes, hence a roughly 50 % larger (absolute) calibration coefficient (-6.5 $K/\delta^{18}O$) was used to take into account the high latitude amplification. In Fig. 4c, d we see that a calibration -6.5 $K/\delta^{18}O$ (i.e. about a 50 % amplification) gives excellent agreement between the this benthic series (bottom) and the *European Project for Ice Coring in Antarctica* (Epica) paleo ice core (Fig. 1b), this is the calibration used in the bottom series of Fig. 1a (shown by the green arrows which give the temperature scale using these calibrations). In any event since glaciation is ultimately temperature dependent, the $\delta^{18}O$ variations over the low frequencies are still

presumably largely temperature driven—even if modulated by geology.

In order to focus on these long time scales, we have constructed Fig. 4d which compares the longer ice cores (Epica, Vostok, only the parts > 1 kyr are shown) with the benthic cores. First, we may note the close agreement of the former with the higher altitude (Huybers, Zachos) benthic cores if the calibration -6.5 K/δ^{18}O is used. With this calibration we have good agreement including the strong change in behaviour from increasing to decreasing RMS fluctuations for periods less than and greater than $\tau_{mc} \approx 80$ kyrs, with fluctuations decreasing in amplitude from about $S(\Delta t) \approx 8$ K (i.e. $\pm$ 4 K) at τ_{mc} to about 2 K ($\pm$1 K) at $\tau_{Mc} \approx 0.5$ Myr. Over this admittedly narrow scale range, the Epica log–log fall off is quite linear (see the reference slope -0.8) suggesting a narrow scaling range that we have tentatively dubbed "macroclimate" in analogy to the macroweather regime to indicate a temporally large scale climate regime (we realize that this term is occasionally used to denote a *spatially* large scale climate zone, but the term will generally be clear from the context). An alternative hypothesis for the range $\tau_{mc} > \Delta t > \tau_c$ is that it is simply a broad maximum associated with the various astronomical forcings which are mainly 41 kyrs (obliquity), 100 and 400 kyrs (eccentricity).

Even if the macroclimate regime is indeed associated with a scaling dynamical mechanism, this would not contradict the presence of at least some periodic responses to astronomical forcings, in particular (Huybers 2007) for example shows a very clear periodic signal (about a factor $\approx$10 above the continuum background) at (41 kys)$^{-1}$, although only over the period $\approx$0.8–2.6 Myrs BP (see the dashed green spike in Fig. 2a). On the other hand, even this particularly strong periodicity only contributes a fairly small fraction of the variance so that we still need to understand the dominant scaling continuum. Reasoning in analogy to the weather/macroweather, we interpret the macroclimate regime as one in which the climate tends to its long term average: for series in the range 10^2–10^5 yrs; although the macroclimate may be what you *expect*, the climate is what you *get*.

If rather than being simply a very broad quasiperiodic spectral maxima, macroclimate is instead a narrow scaling regime, then the new regime starting at about 0.5–1 Myr would be the scale beyond which one typically transitions from one *type* of climate to another, in this case presumably reflecting the increasing importance of geological variability. Indeed, as we go back in time we find that the ice ages cease at the end of the Quaternary $\approx$2.6 Myrs ago. The usual explanation is that due to continental drift, the placement of the continents no longer allowed the accumulation of ice into huge sheets. We dubbed the new lower frequency regime "megaclimate" since "mega" means "large" and the term evokes the megafauna of these ancient climes.

The evidence that the region with $\Delta t > \tau_{Mc} \approx 0.5$ Myr is scaling is more convincing than for the macroclimate regime, in particular the Zachos benthic series (with 14,825 points, see Fig. 4d, see the spectra in Fig. 2a, b) is quite linear out to its limit (67 Myr) and the even longer Veizer series agree well with it at scales 20 Myrs to 553 Myrs ($\xi(2)/2 \approx H \approx 0.4$). The main uncertainty is the region 1–20 Myr where the Huybers series agrees more with one or the other depending on the calibration used, and this may largely be dependent on the role of ice (although see Fig. 5). Whatever the degree to which δ^{18}O fluctuations reflects temperature variations, the fact that it is quite accurately scaling already a significant indicator that the underlying dynamical processes (presumably mostly geological and biogeochemical) have no characteristic scales.

5.3.2 *The δ^{18}O—temperature relation at Myr scales, epoch to epoch variations*

The different δ^{18}O calibrations discussed above assume that the calibration constants are the same at all epochs and vary primarily by latitude. However, it is possible that for a given region, that the calibration depends on the period of interest. For the earlier part of the series where the δ^{18}O—temperature relation is more direct (no ice caps), a calibration of -3.8 *K*/δ^{18}O was suggested (Zachos et al. 2001). Similarly, (Veizer et al. 1999), discusses the overall increasing trend of δ^{18}O towards the present and the hypothesis that this indeed largely reflects cooling trend: some suggest that this has been by as much as 70 K over the 553 Myr series. If it is true that the dynamics affecting δ^{18}O is qualitatively different in the period before or after the early Oligocene, then we would expect the fluctuation statistics to be different. We investigated this directly by breaking the Zachos series into 10 Myr segments, and calculated $S(\Delta t)$ for each. The first three were used to estimate the mean and one standard deviation variation curves for the first 30 Myr (i.e. with the ice sheet sequestering), and the last three were similarly used over the 30–60 Myr period. Figure 5 shows the result: the statistics of the first and second 30 Myr period are systematically within one standard deviation error bar, hence we conclude that their difference is due to normal statistical variability. Therefore, whatever the correct relationship between δ^{18}O and temperature, the statistics have not changed so much and this includes the macroclimate-megaclimate transition somewhere around 0.5 Myr.

5.3.3 *Implications of $H > 0$ for homeostasis and the Gaia hypothesis*

There is no question that the evolution of life on earth transformed the atmosphere, this is the basis of Lovelock's

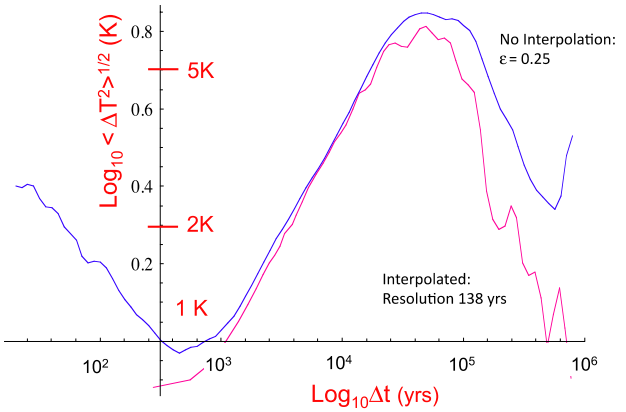

Fig. 6 A comparison of the Epica analysis using a uniform sampling on the linearly interpolated data using the same number of data points as in the original series (5,788 points, interpolated resolution 138 years), magenta, and the result of the interpolation free algorithm described here using $\varepsilon_{min} = 0.25$ (*blue*). The main differences are at the small and large Δt's. The magenta interpolated *curve* is reproduced from Lovejoy (2013)

Gaia hypothesis that posits that just like a living organism, the entire planet displays homeostasis. This means that thanks to negative feedbacks, the earth maintains conditions (including temperatures) in a range fit for life. A famous example—postulated to have operated over the last hundreds of millions of years—is the "CLAW hypothesis" (Charlson et al. 1987, for the authors' initials) which is a negative climate temperature feedback mechanism based on planktonic production of dimethyl sulphide.

But independent of its exact mechanism—by its very definition—negative feedbacks imply that successive temperature fluctuations tend to cancel each other out, i.e. that $H < 0$. However, the proxy evidence from the megaclimate regime is that on the contrary $H > 0$—so that the temperature changes are actually more like drunkard's walks, growing rather than diminishing with time scale. At least for the temperature over the last 550 Myrs, the finding that $H > 0$ is therefore strong evidence against the Gaia hypothesis.

6 Conclusions

The atmosphere has variability spanning nearly 20 orders of magnitude in time, the corresponding spectrum has both continuum as well as quasi periodic features. This poses the question of what is the most appropriate theoretical framework. Starting 40 years ago—at the dawn of current golden age of climate data—the prevailing view has given a central "foreground" role to quasiperiodic processes while treating the remaining continuum as no more than a background noise. This "mental picture" was consecrated in Mitchell's still iconic figure (Fig. 2a) and its updates (Fig. 2c). Using modern data we showed that this picture understates the continuum spectral density by factors of a quadrillion or more. A far more realistic picture of atmospheric variability is obtained by standing this scale bound picture on its head: placing the continuum processes in the fore, with the perturbing quasiperiodic processes in the background. We argued that the continuum is composed of five qualitatively different dynamical regimes: the weather, macroweather, climate, macroclimate and megaclimate (see Figs. 2a, 4e; Table 2), each with unique scaling properties over three or more orders of magnitude in scale and alternating in their qualitative natures primarily due to the signs of their fluctuation exponents (H) but also by their differing intermittencies (characterized by C_1, α, see Table 2). The only potential exception was the macroclimate regime which—being over only a factor of ten or so in scale—might possibly be better represented as a very broad quasi-periodic regime. When $H < 0$, fluctuations tend to cancel, averages converge, the series appear "stable"; when $H > 0$, differences grow with time scale, they appear unstable. For example, we noted that $H > 0$ in the megaclimate regime is incompatible with the dominance of negative feedbacks and hence with the Gaia hypothesis.

This inversion of foreground and background of signal and noise clarifies many aspects of atmospheric dynamics, including the fundamental nature of weather and climate. For example, contrary to Bryson (1997), we have argued that the climate is not accurately viewed as the statistics of fundamentally fast weather dynamics that are constrained by quasi fixed boundary conditions. The empirically substantiated picture is rather one of "unstable", "wandering", high frequency weather processes (i.e. $H > 0$) tending—at scales beyond 10 days or so—and primarily due to the quenching of spatial degrees of freedom (intermediate frequency, low variability)—to macroweather processes. These appear to be stable because positive and negative fluctuations tend to cancel out ($H < 0$).

True climate processes are "weather-like" ($H > 0$) and only emerge from macroweather at even lower frequencies, due to new slow internal climate processes coupled with external forcings (including in the recent period, anthropogenic forcings). These processes presumably include various nonlinear couplings with the fields that Bryson considered to be no more than "boundary conditions" so that "rather than 'boundaries' these become interactive mediums" (Pielke 1998).

Yet, whatever the cause, it is an empirical fact that the emergent synergy of new processes yields fluctuations that on average again grow with scale in at least a roughly scaling manner and become dominant typically on time scales of 30–100 years (somewhat less in the recent period) up to $\approx$ 100 kyrs.

Looked at another way, if the climate really *was* what you expected, then—since one usually expects averages—predicting the climate would be the relatively simple matter of determining the fixed climate normal. On the contrary, we have argued that from the stochastic point of view—and notwithstanding the vastly different time scales—that predicting natural climate change is very much like predicting the weather. This is because the climate at any time or place is the consequence of climate changes that are (qualitatively and quantitatively) unexpected in very much the same way that the weather is unexpected.

Acknowledgments Roger Pielke sr., Gavin Schmidt, Daniel Schertzer and Adrian Tuck are thanked for their useful comments.

Conflict of interest None.

Appendix: An interpolation-free algorithm for estimating Haar fluctuations

Paleotemperatures are typically nonuniformly sampled in time. Sometimes—such as in the case of the Epica series used in Fig. 1b—the problem is due to the compression of the ice with depth and can be somewhat alleviated by sampling the deeper reaches of the core at higher rates (e.g. the high resolution section of the GRIP core shown in Fig. 2b). However, the usual remedy is to interpolate the series and then to resample it at a uniform temporal interval/resolution. While for many purposes this may be adequate, for either spectral or fluctuation analyses it may lead to biases and spurious results. The reason is that interpolation assumes that the curve is not only continuous between points, but also that the series $T(t)$ is differentiable (in the common case of cubic spline interpolation, up to third order!). However in the small scale limit, in a scaling regime, the mean derivatives of order $>H$ diverge. Since we have found empirically that all the relevant atmospheric regimes have $H < 1$, even linear interpolation may give spurious results. Indeed, any linearly interpolated part of the $T(t)$ series will at least locally have $H = 1$ since over such segments, $\Delta T(\Delta t) \approx \Delta t$. Therefore if these regions are too numerous, including the fluctuation statistics over linear segments will introduce biases.

One of the many advantages of Haar fluctuations is that they are quite easy to estimate without any interpolation while accurately taking into account the resolution of the data. We now describe the simple algorithm used in Figs. 4b–e and 5 (note that several of these series were already analysed but using interpolation). Assume that there are N measurements of temperature $T(t_i)$ at time t_i where i is an index 1 through N. Define the running sum S_i:

$$S_i = \sum_{j \le i} T(t_j) \tag{3}$$

Consider an index j and an even number k. The j, k fluctuation $\Delta T_{j,k}$ over the interval $[t_j, t_{j+k}]$ can be estimated as follows. First determine the sums of the $T(t_i)$ over the first and second halves the interval:

$$\Delta S^{(1)} = S_{j+k/2} - S_j; \quad \Delta S^{(2)} = S_{j+k} - S_{j+k/2} \tag{4}$$

in the case of regular sampling, the ratio:

$$\varepsilon = \frac{t_{j+k/2} - t_j}{t_{j+k} - t_j} \tag{5}$$

has the value $\varepsilon = 1/2$.

The Haar fluctuation is simply the average of the first half minus the average of the second half of the interval and can thus be estimated as:

$$\Delta T_{j,k} = \frac{2}{t_{j+k} - t_j}(S^{(1)} - S^{(2)}) \tag{6}$$

However, if ε is too far from 1/2, this estimate may be poor. Therefore, in the calculation of the statistical moments we should only keep the corresponding fluctuations on condition that $\varepsilon_{min} < \varepsilon < (1\text{-}\varepsilon_{min})$ where $0 < \varepsilon_{min} < 1/2$ is a parameter that can be adjusted so as to make the condition as restrictive as we like: exactly uniform sampling corresponds to the limit $\varepsilon_{min} \to 1/2$. Decreasing ε_{min} has the effect of losing precision in the scale Δt, hence it smooths the $S(\Delta t)$ curve. However, taking ε_{min} too close to ½ will result in the rejection of too many fluctuations with the consequence that the statistics will be poor. In the present case, it was found that generally $\varepsilon_{min} = 1/4$ was a reasonable compromise (see Fig. 6). One can check the accuracy by seeing how much the statistics change when ε_{min} is varied (if they don't vary much then the choice of ε_{min} is acceptable). Note also that as usual, the fluctuations are multiplied by an extra "calibration" constant (taken throughout this paper = 2). This ensures that they are quite close to differences in regions where $H > 0$ and close to tendencies (averages with the means removed) in regions where $H < 0$. Once the fluctuations are estimated, $S_q(\Delta t)$ can be estimated by "binning" the fluctuations into "bins" with Δt regular spaced logarithmically. For each bin, the various powers of ΔT are averaged, in our implementation of the algorithm we used 20 bins per order of magnitude in Δt (the software available from http://www.physics.mcgill.ca/~gang/software/index.html).

While the above procedure essentially solves the problem of "holes" in the series, it does not remove possible biases that arise from systematic sampling nonuniformities such as those arising from cores with high temporal sampling rates near the surface and systematically lower rates at depth. When applied to such series, the small Δt part of the $S(\Delta t)$ function will be sampled from the top part of the core where all the high resolution data lie. Therefore the high frequencies will be biased towards the near surface

statistics. However, if the statistics are fairly homogeneous in time—as they typically are (see Fig. 5)—then this is unimportant (see however Lovejoy and Schertzer 2013 for evidence of exceptional Holocene statistics in Greenland).

References

AchutaRao K, Sperber KR (2006) ENSO simulation in coupled ocean-atmosphere models: are the current models better? Clim Dyn 27:1–15. doi:10.1007/s00382-006-0119-7

Ashkenazy Y, Baker D, Gildor H, Havlin S (2003) Nonlinearity and multifractality of climate change in the past 420,000 years. Geophys Res Lett 30:2146. doi:10.1029/2003GL018099

Barras C, Duplessy J-C, Geslin E, Michel E, Jorissen FJ (2010) Calibration of δ18O of cultured benthic foraminiferal calcite as a function of temperature. Biogeosciences 7:1349–1356. doi:10.5194/bg-7-1349-2010

Blender R, Fraedrich K, Hunt B (2006) Millennial climate variability: GCMration of δ18O of cultured benthic. Geophys Res Lett 33:L04710. doi:10.1029/2005GL024919

Bond G, Showers W, Cheseby M, Lotti R, Almasi P, deMenocal P, Priori P, Cullen H, Hajdes I, Bonani G (1997) A pervasive millennial-scale climate cycle in the North Atlantic: the Holocene and late glacial record. Science 278:1257–1266

Bryson RA (1997) The paradigm of climatology: an essay. Bull Am Meteor Soc 78:450–456

Bunde A, Eichner JF, Kantelhardt JW, Havlin S (2005) Long-term memory: a natural mechanism for the clustering of extreme events and anomalous residual times in climate records. Phys Rev Lett 94:048701

Charlson RJ, Lovelock JE, Andreae MO, Warren SG (1987) Oceanic phytoplankton, atmospheric sulphur, cloud albedo and climate. Nature 326:655–661

Charney JG (1971) Geostrophic Turbulence. J Atmos Sci 28:1087

Chekroun MD, Simonnet E, Ghil M (2010) Stochastic climate dynamics: random attractors and time-dependent invariant measures. Phys D 240:1685–1700

Committee on Radiative Forcing Effects on Climate, N. R. C (2005) Radiative forcing of climate change: expanding the concept and addressing uncertainties. National Academic Press, Washington, 224 p

Compo GP et al (2011) The twentieth century reanalysis project. Quart J Roy Meteorol Soc 137:1–28. doi:10.1002/qj.776

Delworth T, Manabe S, Stoufer RJ (1993) Interdecadal variations of the thermocline ciruculation in a coupled ocean-atmosphere model. J Clim 6:1993–2011

Dijkstra H (2013) Nonlinear climate dynamics. Cambridge University Press, Cambridge, p 357

Dijkstra H, Ghil M (2005) Low frequency variability of the large scale ocean circulations: a dynamical systems approach. Rev Geophys 43(3)

Ditlevsen PD, Svensmark H, Johson S (1996) Contrasting atmospheric and climate dynamics of the last-glacial and Holocene periods. Nature 379:810–812

Eichner JF, Koscielny-Bunde E, Bunde A, Havlin S, Schellnhuber H-J (2003) Power-law persistance and trends in the atmosphere: a detailed study of long temperature records. Phys Rev E 68:046133. doi:10.1103/PhysRevE.68.046133

Fraedrich K, Blender K (2003) Scaling of atmosphere and ocean temperature correlations in observations and climate models. Phys Rev Lett 90:108501–108504

Fraedrich K, Blender R, Zhu X (2009) Continuum climate variability: long-term memory, scaling, and 1/f-Noise. Int J Mod Phys B 23:5403–5416

Franzke C (2010) Long-range dependence and climate noise characteristics of Antarctica temperature data. J Clim 23:6074–6081. doi:10.1175/2010JCL13654.1

Franzke J, Frank D, Raible CC, Esper J, Brönnimann S (2013) Spectral biases in tree-ring climate proxies. Nat Clim Change 3:360–364. doi:10.1038/Nclimate1816

Gagnon J, Lovejoy SS, Schertzer D (2006) Multifractal earth topography. Nonlin Proc Geophys 13:541–570

Heinlein RA (1973) Time enough for love. GP Putnam's Sons, New York

Huang S (2004) Merging information from different resources for new insights into climate change in the past and future. Geophys Res Lett 31:L13205. doi:10.1029/2004GL019781

Huschke RE (Ed) (1959) Glossary of meteorology, 638 p

Huybers P (2007) Glacial variability over the last two million years: an extended depth-derived agemodel, continuous obliquity pacing, and the Pleistocene progression. Quat Sci Rev 26(1–2):37–55

Huybers P, Curry W (2006) Links between annual, Milankovitch and continuum temperature variability. Nature 441:329–332. doi:10.1038/nature04745

Isono D, Yamamoto M, Irino T, Oba T, Murayama M, Nakamura T, Kawahata H (2009) The 1500-year climate oscillation in the midlatitude North Pacific during the Holocene. Geology 37:591–594

Kantelhardt JW, Zscchegner SA, Koscielny-Bunde K, Havlin S, Bunde A, Stanley HE (2002) Multifractal detrended fluctuation analysis of nonstationary time series. Phys A 316:87–114

Kolesnikov VN, Monin AS (1965) Spectra of meteorological field fluctuations. Izvestiya Atmos Ocean Phys 1:653–669

Koscielny-Bunde E, Bunde A, Havlin S, Roman HE, Goldreich Y, Schellnhuber HJ (1998) Indication of a universal persistence law governing atmospheric variability. Phys Rev Lett 81:729

Kraichnan RH (1967) Inertial ranges in two-dimensional turbulence. Phys Fluids 10:1417–1423

Lamb HH (1972) Climate: past, present, and future. Vol. 1, Fundamentals and climate now. Methuen and Co, London

Lanfredi M, Simoniello T, Cuomo V, Macchiato M (2009) Discriminating low frequency components from long range persistent fluctuations in daily atmospheric temperature variability. Atmos Chem Phys 9:4537–4544

Lennartz S, Bunde A (2009) Trend evaluation in records with long term memory: application to global warming. Geophys Res Lett 36:L16706. doi:10.1029/2009GL039516

Lindborg E, Tung KK, Nastrom GD, Cho JYN, Gage KS (2010a) Comment on "Reinterpreting aircraft measurement in anisotropic scaling turbulence" by Lovejoy et al. Atmos Chem Phys 10:1401–1402

Lindborg E, Tung KK, Nastrom GD, Cho JYN, Gage KS et al (2010b) Interactive comment on "Comment on "Reinterpreting aircraft measurements in anisotropic scaling turbulence" by Lovejoy, (2009)". Atmos Chem Phys Discuss 9:C9797–C9798

Ljungqvist FC (2010) A new reconstruction of temperature variability in the extra—tropical Northern Hemisphere during the last two millennia. Geografiska Annaler: Phys Geograp 92 A(3): 339–351. doi:10.1111/j.1468-0459.2010.00399.x

Lorenz EN (1995) Climate is what you expect, p 55, aps4.mit.edu/research/Lorenz/publications.htm (16 May, 2012)

Lovejoy S (2013) What is climate? EOS 94(1) 1 January, pp 1–2

Lovejoy, S. (2014a), Return periods of global climate fluctuations and the pause. Geophys Res Lett 41. doi:10.1002/2014GL060478

Lovejoy S (2014b) Scaling fluctuation analysis and statistical hypothesis testing of anthropogenic warming. Clim Dyn. doi:10.1007/s00382-014-2128-2

Lovejoy S, Mandelbrot BB (1985) Fractal properties of rain and a fractal model. Tellus 37(A): 209

Lovejoy S, Schertzer D (1984) 40,000 years of scaling in climatological temperatures. Meteor Sci Tech 1:51–54

Lovejoy S, Schertzer D (1986) Scale invariance in climatological temperatures and the spectral plateau. Ann Geophys 4B:401–410

Lovejoy S, Schertzer D (1998) Stochastic chaos and multifractal geophysics. In: Guindani FM, Salvadori Chaos G (eds) Fractals and models 96. Italian University Press, Italy

Lovejoy S, Schertzer D (2010) Towards a new synthesis for atmospheric dynamics: space-time cascades. Atmos Res 96:1–52. doi:10.1016/j.atmosres.2010.01.004

Lovejoy S, Schertzer D (2011) Space-time cascades and the scaling of ECMWF reanalyses: fluxes and fields. J Geophys Res 116. doi:10.1029/2011JD015654

Lovejoy S, Schertzer D (2012a) Low frequency weather and the emergence of the Climate. In: Sharma AS, Bunde A, Baker D, Dimri VP (eds) Extreme events and natural hazards: the complexity perspective. AGU monographs, Washington, pp 231–254

Lovejoy S, Schertzer D (2012b) Haar wavelets, fluctuations and structure functions: convenient choices for geophysics. Nonlinear Proc Geophys 19:1–14. doi:10.5194/npg-19-1-2012

Lovejoy S, Schertzer D (2012c) Stochastic and scaling climate sensitivities: solar, volcanic and orbital forcings. Geophys Res Lett 39:L11702. doi:10.1029/2012GL051871

Lovejoy S, Schertzer D (2013) The weather and climate: emergent laws and multifractal cascades. Cambridge University Press, Cambridge, p 496

Lovejoy S, Tuck AF, Hovde SJ, Schertzer D (2007) Is isotropic turbulence relevant in the atmosphere?. Res Lett, Geophys. doi:10.1029/2007GL029359,L14802

Lovejoy S, Tuck AF, Schertzer D, Hovde SJ (2009) Reinterpreting aircraft measurements in anisotropic scaling turbulence. Atmos Chem Phys 9:1–19

Lovejoy S, Schertzer D, Tuck AF (2010) Why anisotropic turbulence matters: another reply to E. Lindborg. Atmos Chem Physics Disc 10:C4689–C4697

Lovejoy S, Schertzer D, Varon D (2013a) Do GCM's predict the climate…. or macroweather? Earth Syst Dynam 4:1–16. doi:10.5194/esd-4-1-2013

Lovejoy S, Schertzer, D, Tchiguirinskaia I (2013b) Further (monofractal) limitations of climactograms. Hydrol Earth Syst Sci Discuss 10:C3086–C3090. http://www.hydrol-earth-syst-sci-discuss.net/10/C3181/2013/

Lovejoy S, Varotsos C, Efstathiou MN (2014a) Scaling analyses of forcings and outputs of a simplified Last Millennium climate model. J Geophys Res (under review)

Lovejoy S, Muller JP, Boisvert JP (2014b) On Mars too, expect macroweather. Geophys Res Lett (in press)

Mandelbrot B (1981) Scalebound or scaling shapes: a useful distinction in the visual arts and in the natural sciences. Leonardo 14:43–47

Mann ME, Park J (1994) Global scale modes of surface temperature variaiblity on interannual to century timescales. J Geophys Res 99:819–825

Mann ME, Park J, Bradley RS (1995) Global interdecadal and century scale climate oscillations duering the past five centuries. Nature 378:268–270

Mann ME, Steinman BA, Miller SK (2014) On forced temperature changes, internal variability, and the AMO. Geophys Res Lett 41:3211–3219. doi:10.1002/2014GL059233

Markonis Y, Koutsoyiannis D (2013) Climatic variability over time scales spanning nine orders of magnitude: connecting milankovitch cycles with Hurst-Kolmogorov dynamics. Surv Geophys 34(2):181–207

Mitchell JM (1976) An overview of climatic variability and its causal mechanisms. Quat Res 6:481–493

Moberg A, Sonnechkin DM, Holmgren K, Datsenko NM, Karlén W (2005) Highly variable Northern Hemisphere temperatures reconstructed from low- and high—resolution proxy data. Nature 433(7026):613–617

Monetti RA, Havlin S, Bunde A (2003) Long-term persistance in the sea surface temperature fluctuations. Phys A 320:581–589

Monin AS (1972) Weather forecasting as a problem in physics. MIT press, Boston

Palmer T (2005) Global warming in a nonlinear climate—Can we be sure?, Europhysics news March/April 2005, pp 42–46. doi:10.1051/epn:2005202

Palmer TN (2012) Towards the probabilistic Earth-system simulator: a vision for the future of climate and weather prediction. Q J R Meteorol Soc (in press)

Palmer TN, Doblas-Reyes FJ, Weisheimer A, Rodwell MJ (2008) Toward seamless prediction: calibration of climate change projections using seasonal forecasts. Bull Am Meteor Soc 89:459–470. doi:10.1175/BAMS-89-4-459

Panofsky HA (1969) The spectrum of temperature. J Radio Sci 4:1101–1109

Pelletier JD (1998) The power spectral density of atmospheric temperature from scales of 10**-2 to 10**6 yr. EPSL 158:157–164

Peng C-K, Buldyrev SV, Havlin S, Simons M, Stanley HE, Goldberger AL (1994) Mosaic organisation of DNA nucleotides. Phys Rev E 49:1685–1689

Pielke R (1998) Climate prediction as an initial value problem. Bull Am Meteor Soc 79:2743–2746

Pielke RAS, Wilby R, Niyogi D, Hossain F, Dairuku K, Adegoke J, Kallos G, Seastedt T, Suding K (2012) Dealing with complexity and extreme events using a bottom-up, resource-based vulnerability perspective. In: Sharma AS, Bunde A, Baker D, Dimri VP (eds) Complexity and Extreme Events in Geosciences. AGU, Washington

Pinel J, Lovejoy S, Schertzer D, Tuck AF (2012) Joint horizontal—vertical anisotropic scaling, isobaric and isoheight wind statistics from aircraft data. Geophys Res Lett 39:L11803. doi:10.1029/2012GL051698

Pinel J, Lovejoy S, Schertzer D (2014) The horizontal space-time scaling and cascade structure of the atmosphere inferred from satellite radiances. Atmos Res 140–141:95–114. doi:10.1016/j.atmosres.2013.11.022

Radkevitch, A., S. Lovejoy, K. B. Strawbridge, D. Schertzer, and M. Lilley (2008), Scaling turbulent atmospheric stratification, Part III: empIrical study of Space-time stratification of passive scalars using lidar data. Quart J Roy Meteor Soc doi: 10.1002/qj.1203

Rohde R, Muller RA, Jacobsen R, Muller E, Perlmutter S, Rosenfeld A, Wurtele J, Groom D, Wickham C (2013) A new estimate of the average earth surface land temperature spanning 1753 to 2011. Geoinfor Geostat An Overv 1:1. doi:10.4172/2327-4581.1000101

Rybski D, Bunde A, von Storch H (2008) Long-term memory in 1000-year simulated temperature records. J Geophys Res 113:D02106-02101–D02106-02109. doi:10.1029/2007JD008568

Rypdal M, Rypdal K (2014) Long-memory effects in linear-response models of Earth's temperature and implications for future global warming. Clim Dyn (in press)

Schertzer D, Lovejoy S (1985) The dimension and intermittency of atmospheric dynamics. In: Launder B (ed) Turbulent shear flow 4. Springer, Berlin, pp 7–33

Schertzer D, Lovejoy S (1987) Physical modeling and analysis of rain and clouds by anisotropic scaling of multiplicative processes. J Geophys Res 92:9693–9714

Schertzer D, Tchiguirinskaia I, Lovejoy S, Tuck AF (2011) Quasi-geostrophic turbulence and generalized scale invariance, a theoretical reply to Lindborg. Atmos Chem Phys Discus 11:3301–3320

Schertzer D, Tchiguirinskaia I, Lovejoy S, Tuck AF (2012) Quasi-geostrophic turbulence and generalized scale invariance, a theoretical reply. Atmos Chem Phys 12:327–336. doi:10.5194/acp-12-327-2012

Schlesinger ME, Ramankutty N (1994) An oscillation in the global climate system of period 65–70 Years. Nature 367:723–726

Schmitt F, Lovejoy S, Schertzer D (1995) Multifractal analysis of the Greenland Ice-core project climate data. Geophys Res Lett 22:1689–1692

Schwander J, Jouzel J, Hammer CU, Petit J-R, Udisti R, Wolff EW (2001) A tentative chronology for the EPICA Dome Concordia ice core. Geophys Res Lett 28:4243–4246

Shackleton NJ, Imbrie J (1990) The δ18O spectrum of oceanic deep water over a five-decade band. Clim Change 16:217–230

Shaviv NJ, Veizer J (2003) Celestial driver of Phanerozoic climate? GSA Today, July 2003, pp 4–10

Stolle J, Lovejoy S, Schertzer D (2009) The stochastic cascade structure of deterministic numerical models of the atmosphere. Nonlin Proc Geophys 16:1–15

Stolle J, Lovejoy S, Schertzer D (2012) The temporal cascade structure and space-time relations for reanalyses and Global Circulation models. Quart J Roy Meteor Soc (in press)

Talkner P, Weber RO (2000) Power spectrum and detrended fluctuation analysis: application to daily temperatures. Phys Rev E 62:150–160

Vallis G (2010) Mechanisms of climate variaiblity from years to decades. In: Palmer PWT (ed) Stochstic Physics and Climate Modelliing. Cambridge University Press, Cambridge, pp 1–34

Van der Hoven I (1957) Power spectrum of horizontal wind speed in the frequency range from 0007 to 900 cycles per hour. J Meteorol 14:160–164

Veizer J et al (1999) 87Sr/86Sr, d18O and d13C evolution of phanerozoic seawater. Chem Geol 161:59–88

Veizer J, Godderis Y, Francois LM (2000) Evidence for decoupling of atmospheric CO2 and global climate during the Phanerozoic eon. Nature 408:698–701

Wunsch C (2003) The spectral energy description of climate change including the 100 ky energy. Clim Dyn 20:353–363

Yano J (2009) Interactive comment on "Reinterpreting aircraft measurements in anisotropic scaling turbulence" by S. Lovejoy et al. Atmos Chem Phys Discuss 9: S162–S166. http://www.atmos-chem-phys-discuss.net/9/S162/2009/

Zachos J, Pagani M, Sloan L, Thomas E, Billups K (2001) Trends, rhythms, and aberrations in global climate 65 Ma to Present. Science 292(5517):686–693. doi:10.1126/science.1059412